UNIVERSITÀ DEGLI STUDI DI PADOVA

UNIVERSITA' DEGLI STUDI DI PADOVA

**Dipartimento di Ingegneria Industriale DII**

Corso di Laurea Magistrale in Ingegneria dell'Energia Elettrica

# SAFETY SYSTEMS FOR FLOW AND LITHIUM BATTERIES

Relatore: Prof Andrea Trovò

Laureando: Vudafieri Filippo

Matricola: 1210257

Anno Accademico 2021/2022

# Summary

# Abstract

Energy storage systems assumes a crucial importance for managing the daily fluctuations of power demands in large grids and to cope with the intermittent nature of renewable sources guaranteeing larger proportions of the energy required for grids. Among electrochemical systems, Vanadium Redox Flow Batteries (VRFBs) represent one of the most recent technologies and a highly promising choice. In the first part of this thesis the safety aspects of flow battery systems have been studied. Firstly, an industrial size VRFB "IS-VRFB" with a 9 kW / 27 kWh that is in operation at the Electrochemical Energy Storage and Conversion Laboratory (EESCoLab) has been analyzed regarding safety issues. This part includes the assessment of risks for the environment and the safety of staff in contact with these energy storage systems. The study investigated the known hazards and incidents that can occur during the operational life of a vanadium flow battery storage system and the passive and active protective measures to avoid or contain them. Many standards have also been analyzed to identify the protective measures and test procedures that must be taken to ensure safety. Since, fire risk and personnel safety are paramount considerations when designing, permitting and operating large energy storage systems, it can be concluded that VRFBs are among the safest storage technologies on the grid today. The second part of this thesis consists of an experimental analysis of an in-house designed "Li-ion battery test facility" capable of testing a 48 V Li-ion battery pack composed by 20 cells electrically connected in series with a nominal capacity of 20 Ah. A preliminary experimental campaign has been carried out at the aim to demonstrate the feasibility of this system. This experimental work has been

done within a technology transfer contract between FIAMM Energy Technology and EESColab.

# Introduction

Electrical energy generation has become one of the major topics to reduce $CO_2$ emissions and contain the global warming process; there are a lot of different kind of renewable energy production such as: wind generation, solar, hydroelectric, etc. etc. that have been implemented all around the world but all of them have in common the problem of not being able to guarantee a continuous production [40]. For this reason, Energy Storage Systems (EESs) are studied. Different type of EESs exists: flywheel, pumping hydro, supercapacitors and electrochemical storage system, among these Redox Flow Batteries (RFBs), in particular Vanadium Redox Flow battery, are one of the most promising choice. The most diffuse electrochemical energy storage technology in the present is Lithium Ions Batteries due to their simplicity and high energy density, they are used for both mobile applications, such as smartphones and Electric vehicles (EVs), and stationary use [39]. The EESs are required to respond quickly to variation in the demand of electrical energy required by the grid, they must have a fast response for power balancing requirements, must be able to give enough energy to shave the peaks of load demands, to both release the energy to or absorb from the grid when needed to maintain the electrical energy production of power plants the most possible constant, and must have a capacity high enough to store the excessive energy produced by renewable power plants, storing the energy of a solar power plant during the day and release it during the night when there is no production. Vanadium Battery are studied only for stationary use because they work with a liquid electrolyte stored in two different tanks, as shown in the following chapters, which make them unsuitable for mobile application [41]. Battery Energy Storage Systems (BESSs) can store a high amount of energy in

electrochemical form and thus all this energy can be released into the nearby environment if an incident occurs. Identification and prevention of foreseeable hazards to environment and people are an issue for these systems. The thesis work has been studying and analyzing the possible threats and protective measures for these systems in accordance with the current standards regulation. For VRFBs the possible incidents that can occur during the working life of the battery have been studied. The incidents can be of different nature, electric, fluids leaking and gas generation. For lithium battery the main topic has been the study of Thermal Runaway (TR) behavior since it's the most common cause for lithium batteries incidents and due to its violent and severe behavior many different tests exist, in accordance with standards, to verify a battery safety. Current studies are mainly focused on prediction and prevision methods of Thermal Runaway phenomenon since it's only possible to contain it once it's started. The last part of the thesis work is dedicated to the laboratory test circuitry used for studying the thermal behavior a twenty cells series lithium Ions battery.

# 1 Vanadium Redox Flow Battery

## *1.1 Electrochemical reactions*

Vanadium redox flow batteries are the most diffuse flow battery type as the one who reached effective commercial fruition. A RFB works with positive and negative electrolytic solutions stored in tanks from where they are circulated to the electrochemical cells by means of two pumps. This battery is peculiar because employs the same metal in both half cells, dissolved in aqueous sulfuric acid the negative half-cell employs $V^{2+}/V^{3+}$ redox couple, while the positive half-cell $V^{4+}/V^{5+}$ redox couple. The electrochemical half reactions produced by these solutions in the cells are:

- Positive electrode:
  - Charge: $VO^{2+} + H_2O \rightarrow VO_2^{+} + 2H^{+} + e^{+}$
  - Discharge: $VO_2^{+} + 2H^{+} + e^{+} \rightarrow VO^{2+} + H_2O$
- Negative electrode:
  - Charge: $V^{3+} e^{-} \rightarrow V^{2+}$
  - Discharge: $V^{2+} \rightarrow V^{3+} + e^{-}$

During charging at the positive electrode tetravalent vanadium $VO^{2+}$ ions is oxidized to pentavalent vanadium within $VO^{2+}$ ions, instead at the negative electrode trivalent vanadium $V^{3+}$ ions are reduced to bivalent $V^{2+}$ ions.

## *1.2 Working Principles and components*

In (Fig 1) is shown the scheme of a Vanadium Redox Flow battery. The two active species are stored in the tanks with a determined energy density; the

solution, which is the electrolyte, is sent to the stack by means of two pumps. The minimum flow rate of the pumps must guarantee the finalization of the reactions. The size of the stack defines the powers while the total electrolyte in the tanks defines the total energy.

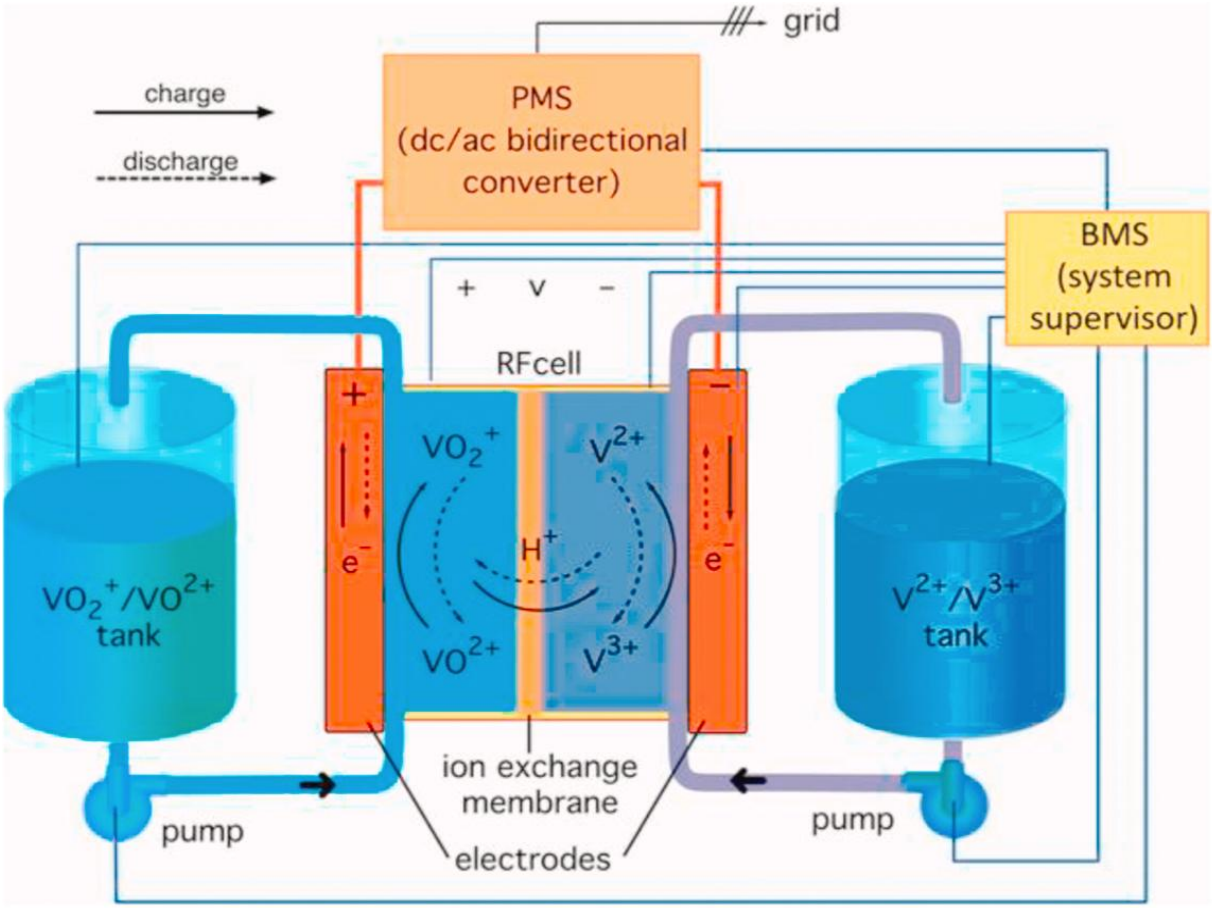


Fig 1_1

Several cells are connected in series to form a stack to produce a useful voltage, while the cell cross sectional area determines the stack current. The electrolyte solution can flow into the cell in two different way [39]:

- Flow-by: the bipolar plates interposed to adjacent cells are designed to have flow channels on each face, to distribute electrolyte to thin electrodes

- Flow-through: the bipolar plates are designed to have flat faces and the electrolyte percolates transversally from one side to the opposite one of thicker electrodes

### *1.2.1 Electrolyte*

In a RFB there are two different types of electrolytes separated by the Ion exchange membrane, one of those is the effective electrolyte while the other is the supporting electrolyte. The electrolyte is the solution that conducts the current through ionization, the supporting electrolyte is the solution who supports the reduced and oxidized forms of the redox couple. The supportive electrolyte also supplies additional ions that increase the solution conductivity and support the flow of the current [40]. Usually, the electrolytes are created by dissolving 0.1M-2M of $VOSO_4$ into 0.1-5M of $H_2SO_4$. It's reported that using 2M of $VOSO_4$ and 2.5M of $H_2SO_4$, the open circuit voltage 1.35V at 50% SOC and 1,60V at 100% SOC [41]. The energy is stored in two different electrolytes in the active materials and to increase the energy density the concentration of the active material must be increased but the problem is that if the concentration of $VOSO_4$ in $H_2SO_4$ exceed 2M precipitation of solid vanadium compounds occurs. $VOSO_4$ occurs in the $V^{5+}$ electrolyte at temperature above 40°C and solid vanadium oxidize in $V^{2+}$ or $V^{3+}$ solution below at a temperature below 10°C. Current studies are looking for effective way to stabilize the electrolytes and inhibit precipitations through adding additives or using mixed electrolyte to enhance the concentration of vanadium, it's speculated that with a sulfuric acid concentration above 5M the vanadium concentration can be increased up to 3M but, so far, no major development has been found [39][40][41].

### *1.2.2 Bipolar Plates and Electrodes*

Bipolar plates are the components that allow the connection in series of individual cells. They have a high cost that can amount to the 50% of the cost of the total cell stack [40]. Common materials are carbon, carbon plastic, graphite, and other materials that all have high electrical conductivity in common. High electrical conductivity leads to lower internal resistance of the stack. The bipolar plate must be made in a material which allows to support the pressure, contact pressure between plate and plate/electrode, applied, it must be high enough to prevent electrolyte leakage but not too high or there will be an excessive electrolyte flow resistance [42]. Metallic materials have also been studied but it has been found that only noble metals are suitable to use because of their intrinsic stability, if a metallic electrode with low chemical resistance is used, metallic ions from the electrode can dissolve into the electrolyte during discharge and corrosion which can cause instability of the chemical equilibrium of the battery [43].

### *1.2.3 Membrane Separator*

Typical separator for Redox Flow Batteries are Ion exchange membrane and are usually in a perfluorinated material and may contribute for 20% of the total cost of the battery. An ideal separator should be able to prevent the mixing of electrolyte and the chemical reaction of the active species [42]. As said in [40]-[44], nafion is the most used and researched material to be used for membranes but the high permeability of active species across the membrane remains a critical problem.

# 2 VRFBs Hazards

The aim of this part of the study is to analyze the possible threats and dangers that can occur while operating with a Vanadium Redox Flow Battery and protection measures that are required to guarantee safety of persons and environment. There are many hazards related to a battery operation and, to analyzed them, they have been divided by their different natures. Which can be summarized:

- Electrical Hazards
- Hazards related to fluids
- Hazards related to gases

Each chapter analyzes first the threat, then provides preventive and/or protective measures that are proposed in the international standards.

## 2.1 Chapter- Electrical Hazards

The electrical hazard related to the operation of a flow battery are the following [10]:

- Direct and indirect contact with live parts of the system (danger of electro-shock)
- Leakage currents
- Short-circuit of the terminals, which can cause an overcurrent that exceed the nominal one

### *2.1.1 Protection against Direct and Indirect Contact*

The FBS is an electrical energy storage device, and, for that, there are hazardous live parts that can cause a risk of electro-shock. The electrolyte

itself must be considered as carrying dangerous voltages. In a flow battery the residual energy, when no electrolyte flow, is limited to the charge storage in electrolyte that remains in the stacks [3]. The fundamental rule for protection against electroshock, according to IEC 61140, is that hazardous live parts must not be accessible and accessible conductive parts must not be hazardous live, neither under normal condition nor under single fault condition [1]. Safeguard guidelines against direct and indirect contact are presented in IEC 60364-4-41 which is based on IEC 61140.

The electrical protective measures that are generally permitted are [8]:

- Automatic disconnection of the supply
- Double or enforced insulation
- Electrical separation for the supply of one item of current-using equipment
- Extra low voltage (SELV and PELV)
- Protection by non-conducting location
- Protection by earth-free potential bonding

As stated in 60364-4-41, protective measures by obstacle or placing exposed parts out of reach shall only be used in installation where access is limited to or under supervision of skilled and instructed person.

### *Protection by disconnection of Supply*

Protection by disconnection of supply is a protective measure where basic protection is provided by basic insulation of live parts or by barriers or enclosures, while fault protection is provided by protective earthing and equipotential bonding or automatic disconnection in case of fault. A protective device shall automatically interrupt the supply under a fault of

negligible impedance between the line conductor and an exposed conductive part of the circuit or a protective conductor, the disconnection time and earthing depend on the connection system:

1. TN: the efficiency of the earthing system of the installation depends on the reliability and effective connection of the protective conductors (PEN or PE) to earth. The neutral-point or mid-point of the supply system shall be connected to earth, or, if none of those are available, shall be directly earthed a line conductor itself. In the presence of a battery installation, usually the negative terminal is earthed, as shown in Fig 2_1. In a stationary installation, a single conductor may serve both as protective and as neutral conductor and no switching or isolating devices shall be inserted in the PEN conductor [1]. Every exposed-conductive part of the installation and of the equipment shall be connected to protective conductor (PE), PEN conductor, or the earthing functional and protective conductor (FPE), to the point of the battery having earth potential which is connected to earthed point of the power supply system. For fault protection, protection against indirect contact, overcurrent protective devices and/or residual current protective devices (RCDs) may be used.

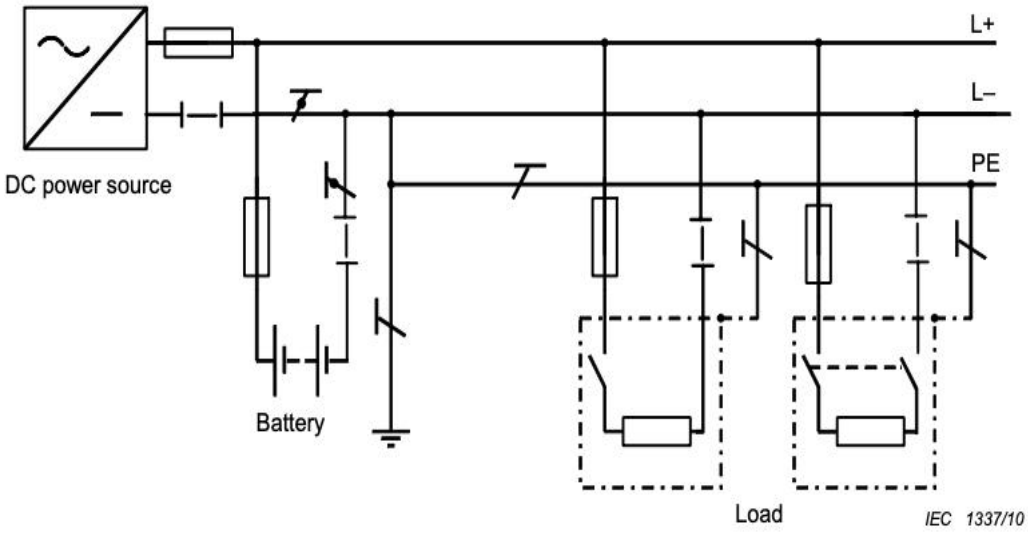


Fig 2_1

2. TT: the neutral-point or mid-point shall be connected to earth, or, if none of those are available, a line conductor shall be earthed. For a battery installation usually is the negative terminal. Every exposed-conductive part protected by the same device shall be connected by the same protective conductor to an earth electrode common to everyone of those parts, as shown in fig 2_2. Simultaneously accessible conductive parts shall be connected to the same earth electrode [8]. Where several protective devices are utilized in series, this requirement applies separately to all the exposed-conductive parts connected by each device. The earth electrode of those parts must be different from the system earth electrode. Generally, in TT systems, RCDs shall be used for fault protection.

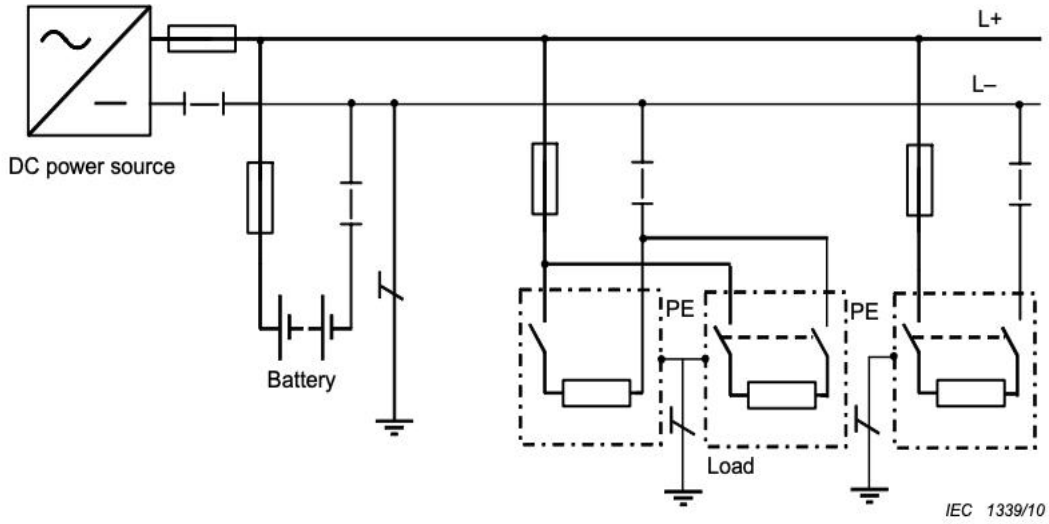


Fig 2_2

3. IT: This system shall be usually insulated from earth or the neutral-point, mid-point or, if those are not accessible, a line conductor shall be connected to earth through a high impedance, fig 2_3. Doing so, in the event of a single fault to an exposed-conductive part or to earth, the fault current is low and then the disconnection of the supply is not required, which is a safety measure that still remains in the event of a second fault to prevent hazardous touch voltage levels. In the case an IT system is used to guarantee continuous supply, an insulating monitoring device and an RCM (residual current monitoring device) or insulation fault location system shall be provided to notify and locate the occurrence of a first fault from a live part to an exposed-conductive parts or to earth. Both these devices shall initiate an audible and/or visual signal of warning that shall continue till the fault of the fault. In the presence of a visual signal the audible one can be neglected [1].

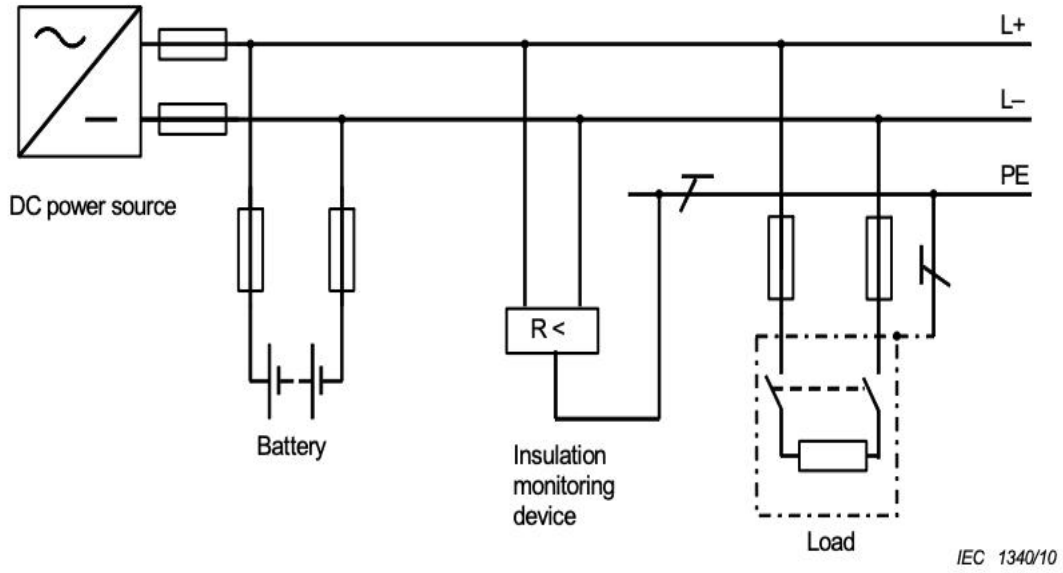


Fig 2_3

Since in Vanadium Flow Battery the electrical energy is stored in acid electrolytes, which are corrosive, every part of the battery that shall be in direct contact with the electrolyte must be made in materials not susceptible to corrosion, typically plastic materials are used. For this purpose, the battery, except for the terminals, is made with non-conductive materials so there is no other part in direct contact with the electrolyte that shall be connected to earth. Therefore, in TT and TN systems it's common use to bound the negative terminal of the battery to earth by a protective conductor and, if necessary, additional earthing of the protective conductor may be required to ensure that it's potential deviates as little as possible from earth potential.

### *Protection by extra Low Voltage*

Protection by extra low voltage is provided by two different systems: Protection Extra Low Voltage (PELV), Safety Extra Low Voltage (SELV) and

Functional Extra Low Voltage (FELV) [1]. These systems are identified as 0 category systems because they provide a maximum nominal voltage of 50 a.c or 120 d.c.[16]. For both SELV and PELV it must be guaranteed electric separation between SELV and PELV circuits and any other circuit who's not of these type and basic insulation between every one of these circuits. For SELV only basic insulation between earth and the SELV system itself must be provided.

Basic and fault protection for SELV and PELV systems is assured to be provided when the following requirements are met:

- The nominal voltage cannot exceed the upper limit of 50V a.c and 120V d.c.
- The sources can be a safety isolating transformer or a source of current that guarantee the same level of safety, an electrochemical one or another source independent of a higher voltage circuit, mobile sources supplied at low voltage or even certain electronic devices that are assured to not exceed the maximum voltage limits [1].
- If the nominal DC voltage of the battery does not exceed 60V d.c. and the above conditions are met, then protection against direct contact can be omitted [8]. In general, in normal dry condition if Vn does not exceed 25V a.c. and 60V d.c and, for PELV only, and every exposed-conductive part of the system is bounded to the main earth terminal through a protective conductor, then basic protection is unnecessary [1]
- If the nominal Voltage, Vn, does exceed 25V a.c. or 60V d.c., or if the equipment is immersed, basic protection shall be provided with insulations and barriers/enclosures in accordance with annex A of [1]. Basic insulation must completely cover the live parts of the circuit and shall be removed only by destruction of itself. Live parts must be

inside enclosures or behind barriers which provide a degree of protection IPXXB or IP2X. If a large opening on the enclosure is required, for functional or maintenance purpose, then suitable precautions must be taken to avoid unintentional contact with live parts, shall operate by or under supervision of skilled personnel. The removal of protection barriers or enclosure shall be possible only with a key or after disconnection of the supply to live parts. Restoration of the supply shall be possible only after the replacement of the safety measures.

Where the Nominal Voltage Vn does not exceed 60V a.c. or 120V d.c but one or more of the above requirements are not met, usually when the source is a common transformer or the circuit is not separated by other circuits who are not PELV or SELV, then the FELV system must be considered [8]. The requirements of FELV systems for basic protection are the safe for basic insulation and barriers/enclosures of the other two systems. Requirements for fault protection are assured when the exposed-conductive parts of the FELV circuit are bounded to earth potential through a protective conductor [1].

### *2.1.2 Short Circuit*

The electrical energy stored in a FBS can be released in an uncontrolled and inadvertent manner due to short-circuit of the terminals. The high energy, and consequentially high currents that can be generated, can produce molten metal, sparks, fire, explosion, and vaporization of the electrolyte [8] [10]. The main connection at the battery terminals shall be designed to withstand the mechanical stress caused by electromagnetic force

generated during a short circuit [8]. The main prevention measure must be considered when designing the battery system because all battery connections, circuit breakers and fuses between stacks, shall be installed in way that short-circuit shall not happen under any foreseeable condition; residual current protective devices shall be able to detect residua d.c. current and to interrupt circuit currents under normal and fault conditions. The behavior of a Flow Battery under fault condition is analyzed in [11]. It has been taken into study a VRFB manufactured by CellCube and operated it under fault conditions looking for critical safety of the system. The studied fault conditions were the following:

- Shorting with a fuse: to simulate a short with fuse blow the stack without electrolyte flow was short-circuited for 8s and then was returned to the state of open-circuit condition after another 8s. IT has been seen that no dangerous temperature has been achieved ate the terminals, no production of sparks, smoke, and the stack cycled normally after the short.
- Full short with no pumping: this case can be happened for example, while decommissioning the battery, it's likely that some of the electrolyte remains in the battery and, in the worst case, all the electrolyte would remain in the stack at a highly charged state. To simulate this event the stack, without pumping, was shorted until the current decreased to insignificance, <0.5 A. It has been seen a rather small rise of the temperature and no unwanted phenomena, so no hazardous behavior has been detected.
- Short-Circuit with pumping: this is the less plausible case because it can happen if a foreign body fell on and connect the terminals while the battery is working, so during maintenance. For this reason, the

wearing of metallic objects and or conductive clothing near FB is prohibited by standards [10]. To simulate this case the stack was shorted for a period of 280s, expecting that that the operator or the battery system would have stop the pumps withing this time. it has been seen no production of smokes, sparks or others hazardous phenomena, the sturdy plastic enclosure didn't show any particular rise in temperature which is instead shown at the terminals and outlet channels. After the test the stack was autopsied and there were no particular signs of damage.

- Internal Short-Circuit: to proceed on this test a 20-cell stack was built with a $3mm^2$ hole in one of the membranes. The stack was then cycled for 24h and autopsied after, it has been seen that the pinhole had not changed size and the membrane shown no sign of overheating, there was no production of sparks or smokes, there was only relatively rapid mass transfer (which could be used to detect this kind of failure in an operating system).

From the study it is found out that the fault current is 50% higher than the nominal one but, even in these conditions there are no dangerous rise of the electrolyte temperature. Or if the rise can be potentially dangerous it is still slow respect to the time of action of the protection devices. If the fault occurs when the battery and pumps are working, the rise of the electrolyte's temperature in the stack is mitigated by the fresh electrolyte that flows in. Anyway, in this study the main hazard aspect that was looked for has been the rise of the temperature, electrical safety is guaranteed simply by use of appropriate fuses. In the end they looked for variations of the life cycle of the battery and, luckily, there are any significant variations, the battery remains fully operative and in the case of internal short-circuit

it's sufficient to increment the hydraulic flow rate to obtain the same performances.

### *2.1.3 Leakage Currents*

To guarantee personal safety and proper operation of equipment in the event of a grounds faults an earthing system is required. The aim is to disperse leakage current in the ground without generating dangerous touch and step voltages and to ensure that potential deviates as little as possible from earth potential for those equipments that can be sensible to disturbs. An earthing system to be aligned with standards must meet the following requirements [2]:

- Must have enough mechanic and chemical resistance (to corrosion)
- Conductors must have a section large enough to carry the current without been damage by the thermal effect
- Must guarantee the preservation of the electrical equipment connected to the system and to the goods around the system
- Step and contact voltages must remain under the limits identified in [2]

to do so the value of the fault current, duration of the fault, ground's impedance and the geometry of the earth disperser, must be taken into account while designing the system [18]. Considering a TT system the earth conductor section value in calculated with the following formula:

$$S = \sqrt{\frac{{I_F}^2 \cdot t}{{k_c}^2}}$$

$k_c$ is a parameter that depends on the conductor material, initial and final temperature

t is the intervention time of the protection

$I_F$ is the fault current, in Ampere, that flow towards earth through the conductor and is calculated by: $I_F = \frac{U_0}{R_E}$ where $U_0$ is the source nominal voltage and $R_E$ is the soil resistivity, which is a parameter that depends on the type of soil and the type of disperser [17]. The Flow Battery is a system where no point of the installation is directly connected to earth, so ground faults are due to leaking of the charged electrolyte from the hydraulic system [8]. Skilled personnel are required to handle the battery, they have to be aware about the risk of electrocution when they come directly in contact with the leaking electrolyte, the person himself become part of the circuit of the leakage current, and the phenomena of arcs and fire when the short-current is established by the leaking electrolyte [3]. When spilling the hydraulic system must be stopped and the leaked electrolyte must be neutralized with appropriate neutralizing material. For maintenance operation is preferable to completely discharge prior to undertake any action to avoid foreseeable dangerous event and use protective clothes that are resistance to corrosion and that can prevent electrostatic discharge, all metallic objects and jewelry must be removed to avoid accidentally short-circuit of the battery terminal and when the nominal voltage exceed 120V d.c insulated protective clothing and local insulated coverings shall be required to prevent personnel making contact with the floor or parts bounded to earth [3]. Only cotton-based clothes moistened with water shall be used for battery cleaning [8]. Even if all the above precautions have been implemented, nothing guarantees the null probability of a ground fault, so for a greater safety can be useful to connect to earth, by a PE, all metallic objects that are allocated in the battery room and, given the hydraulic nature of the fault, a detention leaking sensor shall be implemented. The grounding system is the fundamental protection

system against over-voltages caused by lightning, an efficient earthing can disperse those voltages without damaging the devices connected to the grid [4][5]. There are several studies that analyze this problem, but they take into account only the “design” of the grounding grid to achieve a better dispersion and not the system whose it’s connected [6].

## 2.2 Gases Hazards

Flow Batteries can produce many harmful gases, the type of gas and the rate of production depend on the characteristic of the battery and on the working conditions. It’s the constructor that must give adequate information about gas production. Gases are usually produced in the stacks and accumulated in the system; in FBs they tend to accumulate in the top portion of the tanks [3]. Special attention shall be paid to the production of hydrogen, which can produce an explosive mixture [8].
Table 2.2_1 describes the different risks associated with these gases and a possible protective measure.

Table 2.2_1

| | HAZARDS | PROTECTIVE MEASURES |
|---|---|---|
| EXPLOSIVE GAS | Generation and accumulation of combustible gases | Reduction in the generation of combustible gases |
| | Mixture of gas and oxygen | Dilution of combustible gases |
| | | Prevention of diffusion of gases outside the volume where they are generated |

| | | |
|---|---|---|
| | Presence of ignition sources | Elimination of ignition sources |
| | | Prevention of external oxygen ingress |
| TOXIC GAS | Generation and accumulation of toxic gases | Elimination of toxic gases |
| | | Dilution of toxic gases |
| | Human access to vicinity of toxic gases | Collection of toxic gases by a scrubber |
| | | Limitation to human access |
| CORROSIVE GAS | Generation and accumulation of corrosive gases | Construction of the system with corrosion-resistance materials |
| | | Elimination of corrosive gases |
| | | Dilution of corrosive gases |
| | Human access to vicinity of corrosive gases | Collection of corrosive gases by a scrubber |
| | | Limitation to human access |
| Gases Affecting the Respiratory System (GARS) | Generation and accumulation of GARS | Elimination of GARS |
| | | Dilution of GARS |
| | Human access to the vicinity of GARS | Collection of GARS by a scrubber |
| | | Limitation to human access |

### *2.2.1 Protective Measures against Explosion*

When the FB is charged above the rated voltage range the generation of hydrogen and oxygen increases as a result of electrolysis of the water, these gases are then emitted into the surroundings and when the hydrogen concentration exceeds $4\%_{vol}$ in air, an explosive mixture can be made [19]. There are two parameters to identify an explosive mixture: the Lower Explosion Limit (LEL), that is concentration in air of the flammable gas under

which the mixture cannot explode, and the Upper Explosion Limit (UEL), which above this concentration limit the mixture cannot explode. For hydrogen are respectively 4% and 75%. When the flammable gas concentration in air is in the range identified by these two parameters the necessary conditions for an explosion are met. To trigger the explosion one of the following ignition sources is needed: [20]

- Electric discharge
- Electrostatic discharge
- Atmospheric discharge
- Mechanically generated sparks
- Hot surfaces
- Exothermic reactions
- Free flames
- Pressure impulses
- Electromagnetic waves
- Ionizing rations
- Ultrasounds

Particular attention must be paid to the generation of electrostatic fields in the near proximity of the region where the explosive mixture is generated. Electrostatic discharges are usually generated by plastic tools, synthetic fibers, insulating clothes and other materials than can build up a charge through rubbing, that's caused by the so-called triboelectric effect, for this reason clothes that can prevent electrostatic discharge must be used for maintenance.

### *2.2.2 Hazardous Area Identification*

One of the measures against explosion is the correct identification of the danger level of the site; the place can be classified in [19][21]:

- Area 0: area where an explosive mixture persists frequently or for a long time
- Area 1: area where in normal working condition an explosive mixture usually persists
- Area 2: area where in normal working condition an explosive mixture doesn't persist

These definitions refer to a one-year period

The requirements for the classification of each area are summarized in the following table 2.2_2

| AREA | Persistence of the explosive mixture | Frequency in a year (In 365 days) | duration |
|---|---|---|---|
| 0 | frequently | $P>10^{-1}$ | d>1000 h |
| 1 | occasionally | $10^{-1}>P>10^{-3}$ | 1000 h>d>10 h |
| 2 | Shouldn't happen | $10^{-3}>P>10^{-5}$ | 10 h>d> 0.1 |

Table 2.2_2

These areas are identified through the type of emission source (SE) and the housing system's ventilation. The SE are divided in 3:

- Continuous degree emission: an emission that is continuous or persist for a long time
- First degree emission: a periodically and predictable emission
- Second degree emission: a not predictable and/or very short emission

A continuous emission source can be the surface of a fluid [19], but since in a flow battery gases should be generated by overcharges and not during normal working condition and since the sulfuric acid electrolyte is not directly flammable, then it could be considered as a first or even second degree emission. It shall be wise to run laboratory tests to determinate the emission degree since it's the manufacturer duty to provide to consumers the ventilation requirements. Ventilation is a protective measure that have the purpose to lower the danger level of an area, it's classified by its capability of lowering the danger, it's classified in: High degree if it's able to lower the SE concentration under the LEL instantly and then as result the danger area is small in extension, Medium degree if the ventilation is capable of maintaining the SE concentration under the LEL and/or the explosive mixture persist for a small period of time, Low degree if ventilation is not able to affect the emission [19].

### *2.2.3 Ventilation Requirements*

Ventilation can be natural or forced, natural ventilation is assured when the installation is outdoor or in an indoor space with enough opening to assure an adequate value of air velocity. For natural ventilation a constant value of air velocity of $w_a = 0.5\, m/s$ is assumed [19][20]. Forced ventilation is required when there the air velocity $w_a$is not reached, usually in indoor spaces but in some rare case even in outdoor spaces, anyway it's a calculation that must be verified directly in the installation site. To proceed in the analysis the gas emission rate $Q_g$must be calculated:

$$Q_g = S \cdot p \cdot c_d \cdot \sqrt{\frac{M}{R \cdot T} \cdot \frac{2 \cdot \gamma}{\gamma - 1} \cdot \left[1 - \left(\frac{p_0}{p}\right)^{\frac{\gamma-1}{\gamma}}\right]} \cdot \left(\frac{p_0}{p}\right)^{\frac{1}{\gamma}} \text{ [21]}$$

Where:

S is the area of the SE

P is absolute pression of the point of the emission

$c_d$ is the efflux coefficient

M is the molar mass of the flammable substance

R= $8314 \frac{J}{kmol \cdot K}$

T absolute temperature on the point of emission

$\gamma$ polytropic index of adiabatic expansion

$P_0$ absolute pressure immediately after the container exits

the air changes in the volume affected by the emission must be evaluated, they are calculated by:

$$C_0 = \frac{Q_0}{V_0} \ (s^{-1}) \ [20]$$

Where:

$Q_0$ is the ventilation rate

$V_0$ is the Volume that is affected by the gas emission.

$$C_0 = \frac{Q_0}{V_0} \ (s^{-1}) = \frac{w_a \cdot {L_0}^2}{{L_0}^3} = \frac{w_a}{L_0} \ [19 - 21]$$

Where $L_0$ is the edge of a fictitious cube of the same volume as $V_0$. To determinate $L_0$ the danger distance $d_z$ must be calculated:

$$d_z = k_z \left( \frac{42300 \cdot Q_g f_{SE}}{M \cdot k_{dz} LEL_v w_a} \right)^{0.55} \quad [20][21]$$

The danger distance defines the distance from the SE where the gas concentration is below $k_{dz} LEL_v$.

$M$ is the molar mass of the flammable substance.

$LEL_v$ in volume percentage.

$k_{dz}$ is a coefficient that varies from 0.25 to 0.5 for continuous and first-degree emission and from 0.5 to 0.75 for second-degree emission [20].

$k_z$ is a coefficient that is equal to 1 for outdoor spaces and varies according to $\frac{X_m\% \cdot f_{SE}}{k \cdot LEL_v}$ for indoor spaces [20].

$f_{SE}$ is the dilution factor, from 1 for good to 5 for bad dilution capability.

$X_m\%$ is the average concentration in the indoor space, known as far-field concentration.

For hydrogen emission in indoor spaces $k_z$ has the values reported in table 2.2-3.

| $\frac{X_m\% \cdot f_{SE}}{k \cdot LEL_v}$ | $k_z$ |
|---|---|
| <0.1 | 1 |
| From 0.1 to 0.4 | 2 |
| From 0.41 to 0.75 | 3 |
| From 0.76 to 0.9 | 4 |
| From 0.9 to 1 | 5 |

Table 2.2_3

Where k is a safety factor of 0.25 for continuous and first-degree emission and 0.5 for second-degree emission.

$L_0$ is defined as: $L_0 = k_0 \cdot a \cdot D_{SE}$ where a is at least equal to $d_z$ and means the extension of the danger area [20][21].

$k_0$ is a coefficient usually equal to 2 and $D_{SE}$ is the maximum linear extension of the SE.

The necessary air flow to maintain the flammable gas concentration under the $k \cdot LEL$ limit is calculated with the following formula:

$$Q_{a\,min} = \frac{Q_g}{k \cdot LEL_m} \cdot \frac{T_a}{293}\ [20]$$

Where $LEL_m$ is the LEL express in the mass $\left(\frac{kg}{m^3}\right)$ and $T_a$ is the room. Temperature.

Another fundamental parameter is the persisting time of the explosive mixture after the source has stopped emitting, it's calculated by the following formula:

$$t = \frac{-f_{SE}}{C_0} \cdot \ln \frac{k \cdot LEL_v}{X_0\%}\ [20]$$

where $X_0\%$ is the initial concentration.

The CEI standard 60079-10-2 for explosive atmosphere and the CEI 31-35 [21] provide formulas to calculate the parameter under many emission's conditions, the ones that are presented in this study are those that refer to sub-sonic emission because the gases are generated form the electrolyte surface.

## 2.3 Liquids Hazards

The hazards related to the leaking of the electrolyte can be divided into:

- Toxicity
- Corrosiveness
- Environmental impact
- Flammability

Prevention measures shall be considered in the design phase to prevent any foreseeable leaking event, but in a fault event the leakage could continue unattended in case the detection system of the leakage is unappropriated. To limit the risk the basic protection that can be implemented are the following:

- Ensuring the sealing performance of the fluid system
- Use corrosion-resistance materials for those parts that are in contact with the electrolyte
- Detecting leakage and predispose safety guard devices (use a leakage sensor)
- Preventing leakage into the surroundings
- Providing information and marking concerning fluids

The FBS must be put in a collecting tray which must have volume at least equal to the larger tank size and must be made in a corrosion-resistance material. The basin serves to prevent the leakage in the surroundings area. Since different chemistry of FBS are currently under development, the manufacturer should inform about specific hazards that are inherent to that product, in particular information about primary emergency for:

- Direct contact and contaminations of persons
- Environmental contamination

Safety datasheet should be provided as well, that shall indicate proper protective clothes for operating with the battery such as: corrosion resistance, not inflammable, resistant to heat, insulating and that can't allow electrostatic discharge. For FBS that operate with sulfuric acid as electrolyte the manufacturer must provide information about percentile concentration of the substance and in the event of a leakage to neutralize the acid sodium carbonate, sodium bicarbonate, sodium hydroxide shall be

used with caution. In the event of fire the electrolyte is not flammable and for that it's safe to use the most adequate extinguish medium, but in the case of both fire and a leakage it shouldn't be use water but instead carbon dioxide shall be use to not disperse the electrolyte in the surrounding area [21]. If a battery operates with different fluids the pipes shall be clearly identified with the name of positive and negative fluid. Mechanical resistance over temperature, pressure and aging must also be considered when choosing the materials.

## 2.4 Housing requirements

Batteries shall be housed in protected accommodations that protects from:

- External hazards e.g. fire, water, shock, vibration, vermin
- Hazards caused by the battery itself
- Access by unauthorized personnel
- Extreme environmental influences e.g. temperature, humidity, airborne contamination

If the ventilation requirements are not met than an adequate ventilation system must be provided. In the housing room or on the exterior of the enclosure, if it's an outdoor installation, warning labels must be placed. The labels must be of the appropriate symbols as specified below [15]:

a) Safe condition: green square
b) Fire protection: red square
c) Mandatory: blue circle
d) Warning Hazards: yellow triangle

To allow emergency evacuation an unobstructed escaped path must be maintained all time with a minimum width of 600mm.

# 3 Lithium Ion Battery

Batteries are dived in two categories: primary and secondary. Primary batteries are those who are for single use only, they have higher energy concentration but are not rechargeable. Secondary batteries are those who are rechargeable, lithium ions are the most famous of this type. They are famous because they are the most common, they have been implemented on mobile devices, Electric Vehicles and up to industrial stationary use and for this reason there is specific regulation for these batteries. During battery operation a large amount of heat is produced from joule effect and chemical reaction of charge/discharge process by the shuttling of $Li^+$. If the heat is excessive or cannot be adequately removed, then the so-called Thermal Runaway phenomenon can occur, which is a very dangerous and irreversible phenomena that cause smoke, fire and even explosion, irreversible for the battery and highly hazardous for personnel and environmental safety.

## *3.1 Thermal Runaway (TR)*

Thermal Runaway, or TR, is a completely irreversible and uncontrollable phenomenon that affects Lithium Batteries and, due to its huge impact and severity, there are many studies that look for the possible causes.

There are five types of cause for this phenomenon:

- Uncontrollable heat generation
- Separator defects
- Mechanical abuse
- Thermal abuse
- Electrical abuse

### *3.1.1 Uncontrollable heat generation*

Excessive internal heat generation can cause oxygen release from the cathode material, which can directly create an explosive mixture in nearby surroundings and can lead to numerous exothermic side reactions generating more heat.

### *3.1.2 Separator defects*

Separator defects create internal short-circuit paths and rapid discharge of the energy stored, accompanied by uncontrollable chain reactions and release of a huge amount of heat.

### *3.1.3 Mechanical abuse*

Lithium Ion are the most common batteries implemented on electric vehicle (EV), with the increase in the number of EVs on the roads there is also an increase of accidents that concern EVs and mechanical abuse usually identify the damage and the subsequent consequences of the battery of an EV in presence of a collision. The outer shell of the battery provide the first protection against thermal and mechanical abuse, the casing has to be able to withstand high local temperature, mechanical force and ensure that the internal structure is not damaged. Under specific limits of temperature and mechanical force. The mechanical behavior of the outer casing is the most vulnerable point of the battery in case of accidents and upon damage air can flow inside, reacting with active components and electrolytes [24]. Even if the shell is only deformed, the battery's internal component can be severely damaged, the internal structure can be completely broken up to directly connect the terminals generating a full internal short-circuit, or in

case only some parts are damaged can generate a local short-circuit anyway, both these events can trigger TR phenomenon. Mechanical abuse is a hazard mainly bound to EVs batteries, for batteries predisposed for stationary used physical and mechanical accidents should be very rare or even unthinkable events, so for stationary Lithium-Ion batteries the battery rooms shall be provided with safety measures against fall or other mechanical dangers but the mechanical abuse is on a lower hazard level than electrical and thermal abuse.

### *Internal Short Circuit*

Internal Short Circuit (ISC) happen If the internal structure of the battery gets ruptured or deformed enough to directly connect the terminals, this can be caused by incidents, impact or other form of mechanical abuse but also in the presence of a defective product, in every case an ISC is the main known trigger for TR phenomenon. The nail penetration is the most well known test to study a battery's behavior in the occurrence of an ISC. Shan Huang et al. [29] studied the behavior of commercially available Li-ion pouch cells with nominal capacity of 3 Ah (LP 6050100, Tenergy) and of 20 mAh (PGEB0052081, Powerstream Technology), these batteries have been tested individually or in a module for a total of seven tests, these tests are reported in the following table.

| Test | Cell/electrode information | Nail diameter | Penetration speed | note |
|---|---|---|---|---|
| 1 | 3 Ah cell | 3.00 mm | 40 mm•$s^{-1}$ | Full penetration |
| 2 | 3 Ah cell | 1.27 mm | 0.02 mm•$s^{-1}$ | Full penetration |
| 3 | 20 mAh single-unit cell | 1.27 mm | 0.02 mm•$s^{-1}$ | Penetration from Cu to Al |
| 4 | 20 mAh single-unit cell | 1.27 mm | 0.02 mm•$s^{-1}$ | Penetration from Al to Cu |
| 5 | 3-cell module made by 3 Ah cells | 1.27 mm | 0.02 mm•$s^{-1}$ | Full penetration |
| 6 | Cathode on Al foil | 1.27 mm | 0.02 mm•$s^{-1}$ | From cathode to Al |
| 7 | 7 Ah dummy cell | 1.27 mm | 0.02 mm•$s^{-1}$ | Partial penetration |

Table 3.1_1

Test 1 was conventional nail penetration test, test 2,3,4,5 were 3S nail penetration of respectively 3 Ah cell, 20 mAh cell, of a module of three 3 Ah cells connected in parallel. Test 6 was penetration of a single cathode coated in an aluminum foil and test 7 was 3S penetration of a dummy cell,

without electrolyte, that was later examined by X-ray microscopic imaging. 3S penetration identify a type of procedure where the nail is small in diameter with the purpose to reduce influences of nail on Thermal Runaway behavior, the penetration speed is low enough to enable to control penetration depth and allowing to cause even single layer ISC, a thermal sensor is attached to the nail providing in situ sensing temperature at the ISC spot [30].

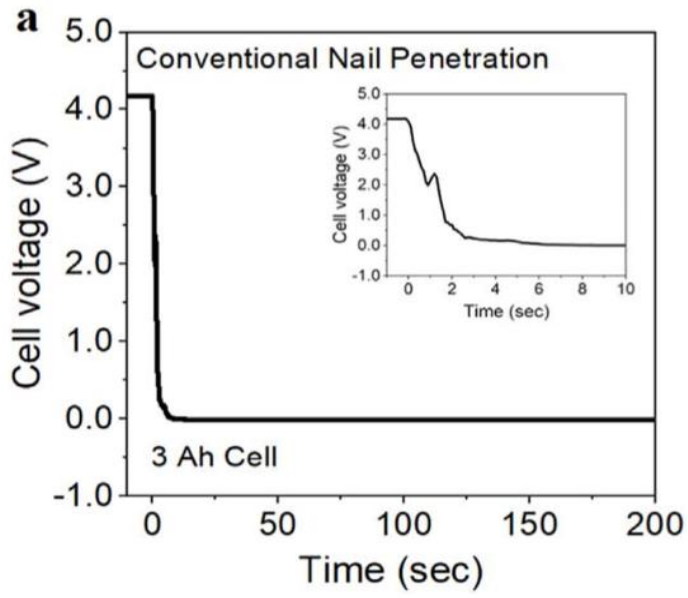


Fig 3.1_1 a and b

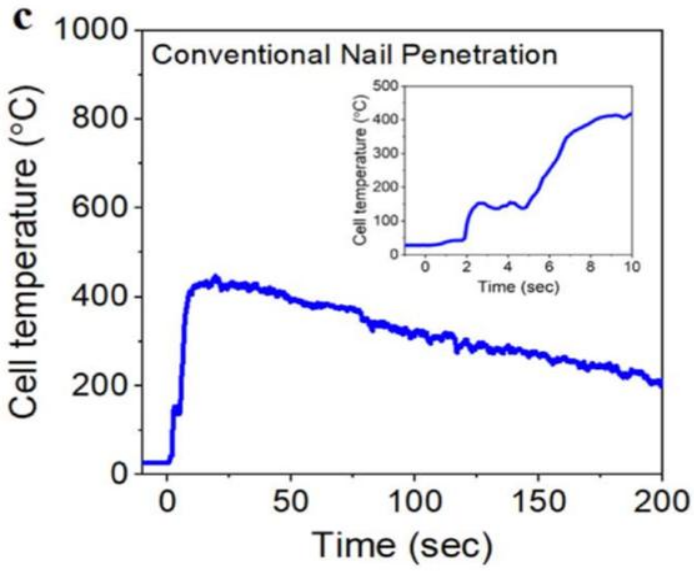

Fig 3.1_1 a,b show the voltage and thermal behavior of the conventional nail penetration test (test 1). It can be seen that the voltage dropped to 0.5 V in 2 s and 0.1 in 5 s while, the surface temperature reached 150 °C in 5 s and reached the maximum temperature, over 400 °C, in 20 s. The battery entered quickly in the Thermal Runaway state, the cell had a thickness of 6 mm and the penetration velocity was 40 mm•$s^{-1}$, it was fully penetrated in 0.2 s, after the peak the temperature decreased with time because of the gradual extinguishment of electrolyte and active materials needed for the TR process.

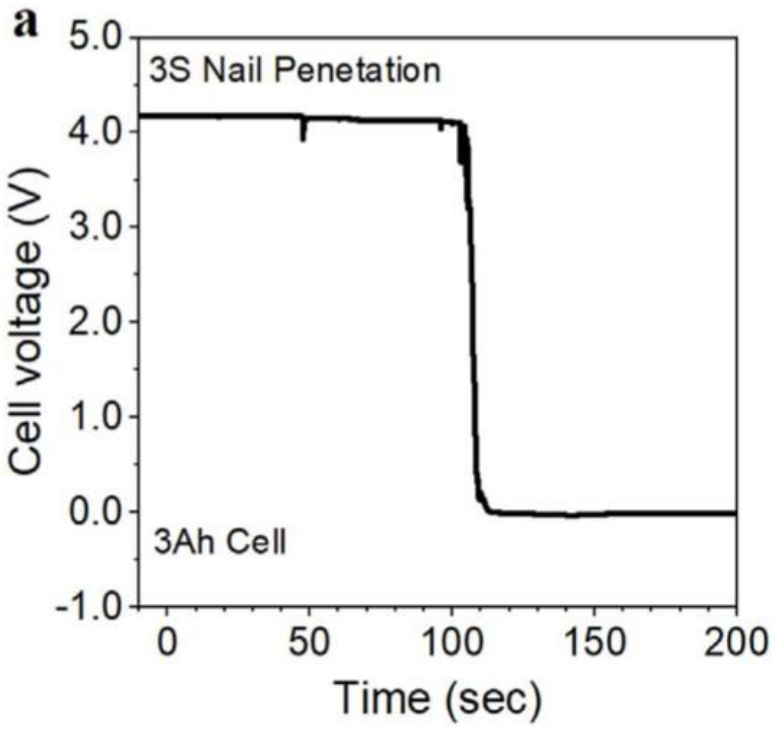


fig 3.1_2 A

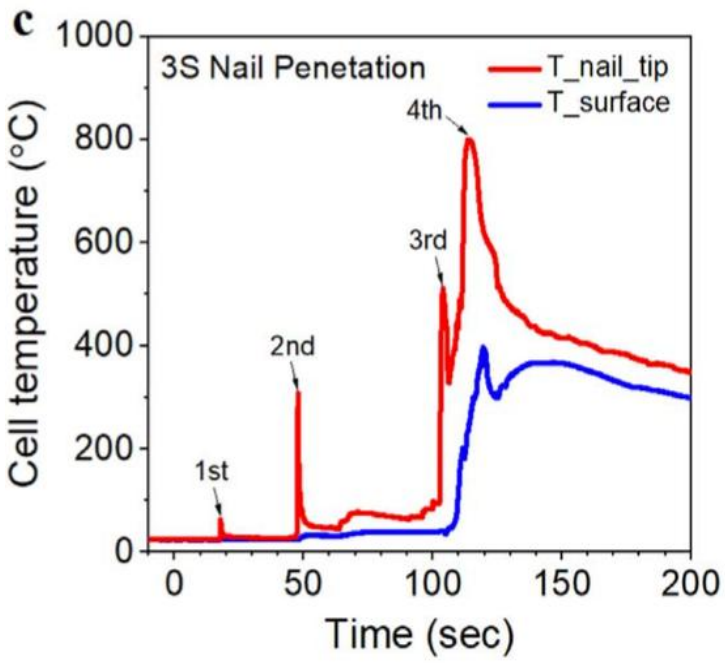


fig 3.1_2 B

Fig 3.1_2 A and B show the voltage and thermal behavior of 3S penetration. It's seen that the TR event begun at 100 s and even the cell voltage needed 100 s to drop, much later than the previous test. The nail had a speed of 0.02 mm•$s^{-1}$ and needed 30 s to fully penetrate the 6 mm thick cell. These graphs suggest that the penetration speed directly affect the TR phenomenon. From the 3S penetration can be seen that the local temperature, at the ISC spot, is much higher, 800 °C, respect to the surface temperature and that there were three peaks before the triggering of the TR phenomenon. The second and the third were above 300 °C and 500 °C, significantly higher than typically TR onset temperature. The nail tip temperature dropped after each peak suggesting that the local heat generation must be dramatically reduced, the heat generation directly depends on the ISC current, so it's hypothesized and abruptly drop of the

current. The 3-cells module was tested to prove this hypothesis, the cells . As shown in Fig 3.1_3 the individual cell current had peaks corresponding to the temperature peaks and between these peaks the current was nearly zero. This finding supports the hypothesis because a short pulse of current can cause a pulse heat generation.

Fig 3.1_3 A and B

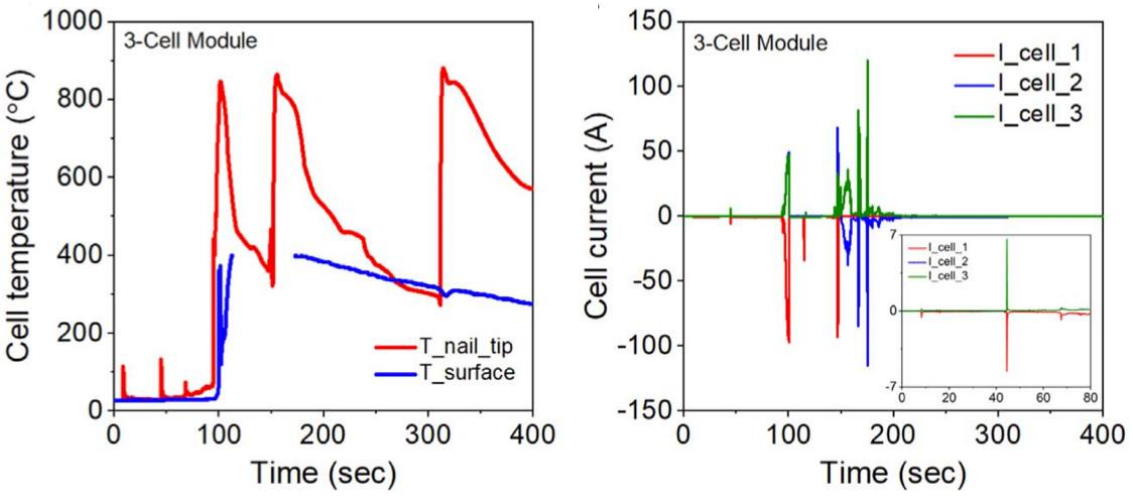


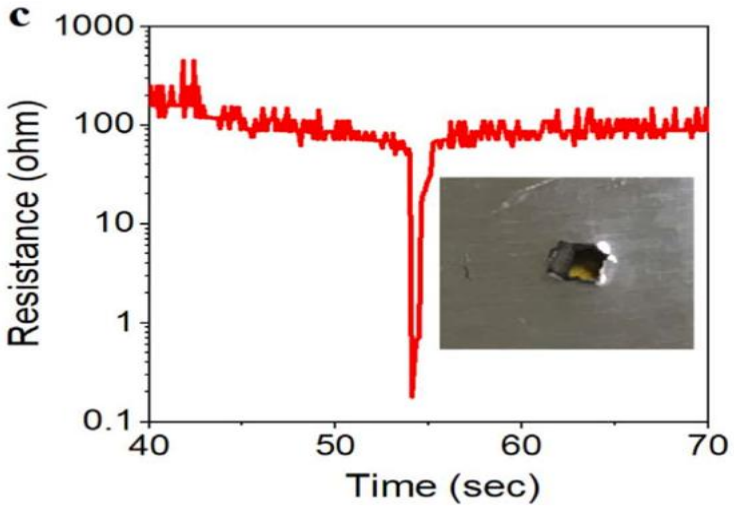


fig 3.1_4

Test 6, a single layer cathode coated in an aluminum foil nail penetration, was done to analyze the understand the variation of ISC resistance. The

behavior is shown in Fig 3.1_4.the resistance dropped of several orders of magnitude when the nail touched the aluminum foil and then returned to a value equal to the one previous the drop. It's suggested that the sudden increase after the drop is due to the rupture of the aluminum foil, but nonetheless support the previous hypothesis because the sudden ISC current peak can be caused by a sudden ISC resistance drop. Huang et al. proposed a mechanism of interpretation for those three different ISC peaks, the first peak is due to the nail making direct contact between the cathode, the anode and the copper foil, as shown in Fig 3.1_5

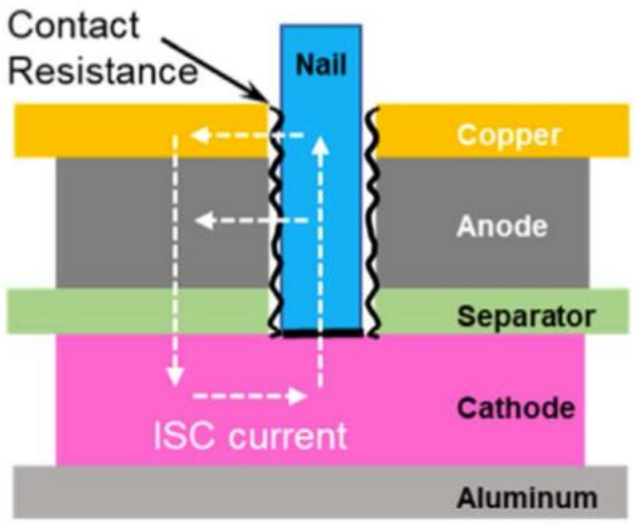


Fig 3.1_5

High resistance of cathode material would limit the ISC current. The second peak is due to the direct contact of the nail with the aluminum foil, the aluminum resistance is very small, respect to the cathode resistance, and also the contact resistance would be small due to tight contact. The ISC resistance would be smaller of several orders of magnitude than that of the previous peak, leading to a high ISC current that causes rapid local heat generation. After that, it's the aluminum foil to be penetrated, the contact resistance between the foil and the nail would be comparable to the

Fig 3.3_5 phase. The rapid temperature drop after each peak can be attributed to temporary stop of internal current and for Huang et al. this suggests that 3S nail penetration method can separate ISC from Thermal Runaway and that increasing contact resistance and/or anode material resistance during an ISC can enhance the battery's safety. Zonghou Huang et al. in [31], studied the behavior of (cathode) $LiFePO_4$ batteries, considered the safest, during nail penetration. The batteries used for the test are 18650 commercial types with a nominal capacity of 1500 mAh and voltage 3.6 V. They conducted different tests to analyze the effects of SOC, penetration speed and penetration depth, the tests details are reported in the following table.

| Test Type | SOC (%) | Penetration Depth (mm) | Penetration Speed ($mm \cdot s^{-1}$) | Nail Diameter (mm) |
|---|---|---|---|---|
| SOC | 0 | 18 | 20 | 3 |
| SOC | 50 | 18 | 20 | 3 |
| SOC | 75 | 18 | 20 | 3 |
| SOC-SPEED-DEPTH | 100 | 18 | 20 | 3 |
| SPEED | 100 | 18 | 10 | 3 |
| SPEED | 100 | 18 | 30 | 3 |
| SPEED | 100 | 18 | 40 | 3 |
| DEPTH | 100 | 6 | 20 | 3 |

| | | | | |
|---|---|---|---|---|
| DEPTH | 100 | 9 | 20 | 3 |
| DEPTH | 100 | 12 | 20 | 3 |
| DEPTH | 100 | 15 | 20 | 3 |

Table 3.1_2

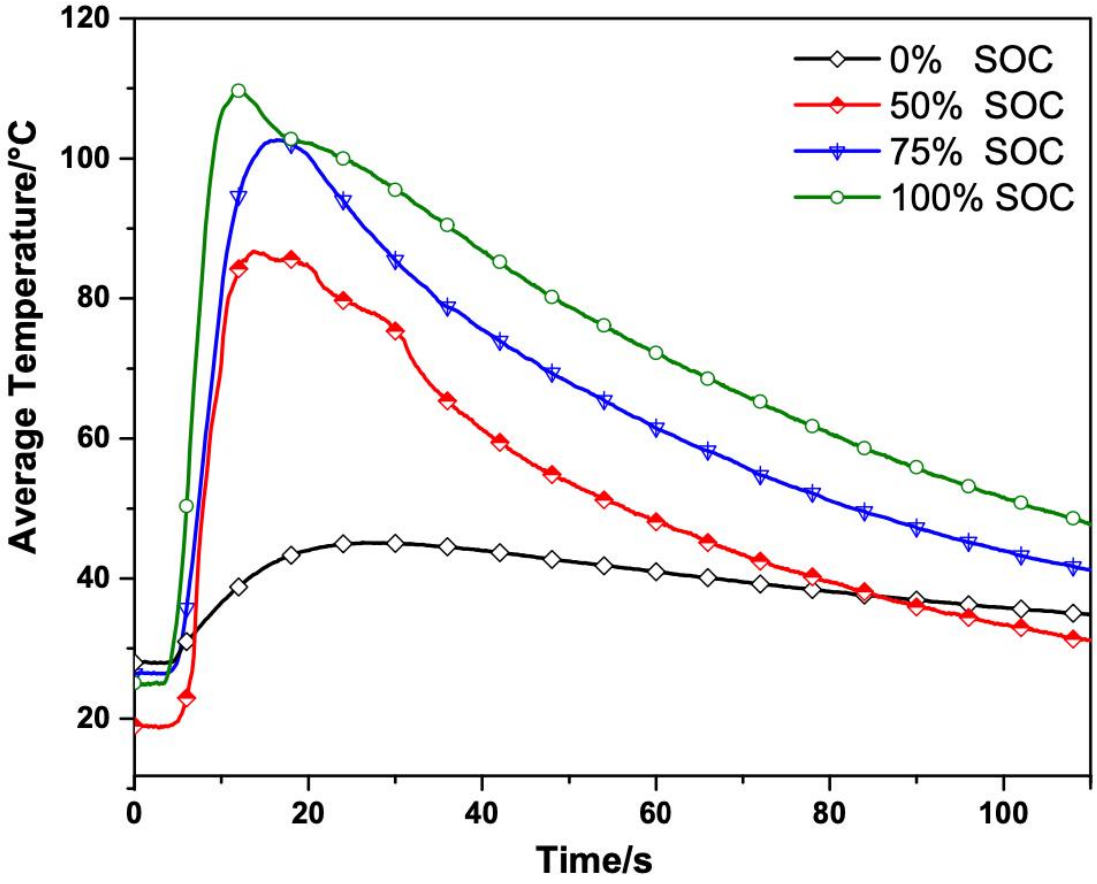


Fig 3.1_6

They first analyzed the SOC effect on the TR phenomenon, four group of batteries were charged to 0%, 50%, 75%, 100% SOC and the thermal behavior is shown in Fig 3.1_6. It's seen that the temperature peak is around 20 s for all the batteries, the battery with 0% SOC has a low temperature peak due to the low electrical quantity, the battery with 100% SOC has the highest peak, who is about 110 °C, while the 75% has a

temperature peak lower than that of the 100% SOC battery and higher than that of the 50% SOC battery. These results show that the higher the SOC, the higher is the overall temperature during nail penetration and this is due to the fact that there is a greater amount of energy stored and instability of the electrodes at higher SOC. From a macroscopic point of view, only leakage occurred in the 0% SOC battery. Leakage, open of the safety valve and a small white smoke generation occurred for the 50% and 70% SOC batteries. Leakage, open of the safety valve and considerable generation of white smoke has been observed for the 100% SOC battery. The batteries, apart for that of 0% SOC, entered TR stage but their behavior was much safer and controlled than others ternary batteries which usually enter TR stage with eject sparks, flames due to the extremely high temperature and active materials. The $LIFePO_4$ stability is due to the inhibition of oxygen loss by strong P-O covalent bonds in the cathode, lowering the oxygen available limits the electrolyte that can be ignited. Penetration speed is also a crucial variable that has been studied, the chosen velocities were 10, 20, 30, 40 $mm \cdot s^{-1}$ and the batteries thermal behavior is shown in Fig.07.

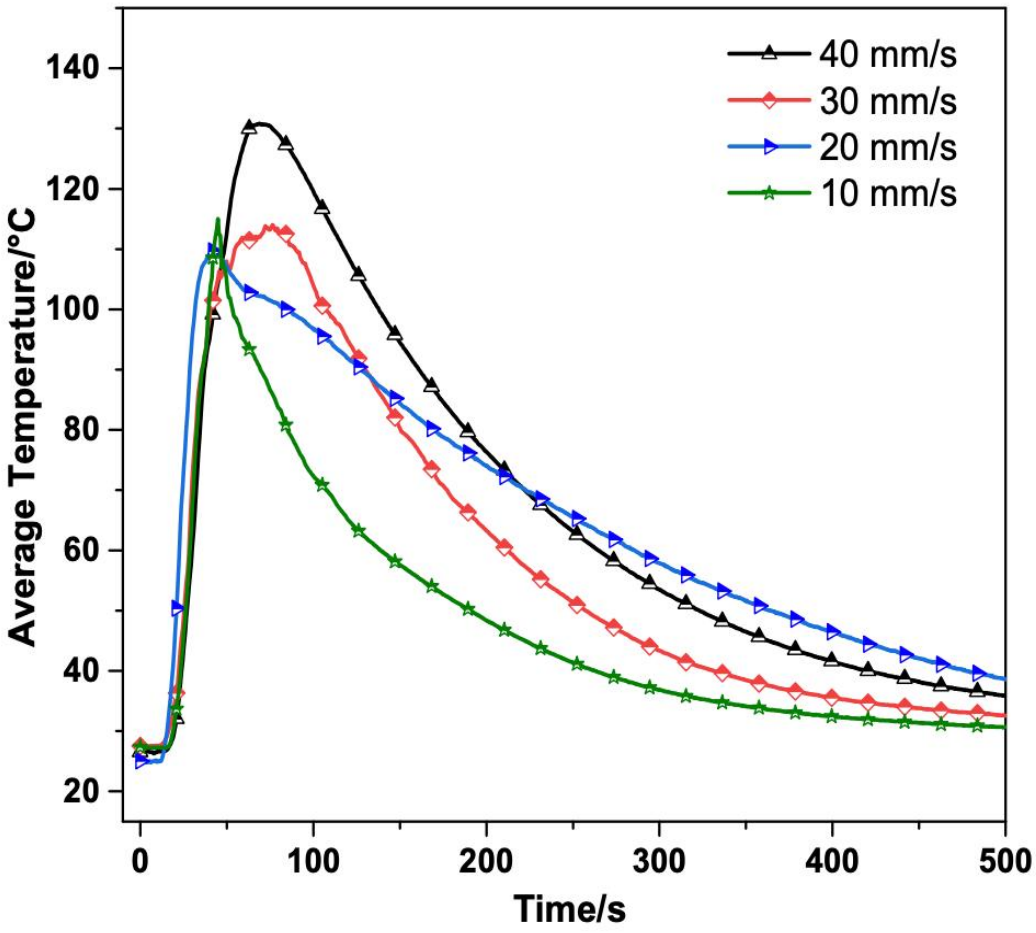


Fig 3.1_7

The batteries tested were all pre-charged at 100% SOC. As can be seen from Fig.07 all batteries reached temperature peak around 70 s and all batteries experienced Thermal Runaway. The TR phenomenon behavior for $LiFePO_4$ was the same as that of the SOC test, no violent phenomena, no sparks and no flames, the safety valve opened to release a great amount of white smoke. The tests showed that penetration speed do not affect TR behavior greatly but form Fig.07 it's seen that higher penetration speed brings higher average temperature, with a peak of nearly 130 °C for 40 $mm \cdot s^{-1}$. Huang et al. found that penetration depth is a more crucial aspect for Thermal Runaway phenomenon, they have done five different penetration depth (6, 9, 12, 15, 18 mm) tests on batteries charged at

100% SOC, starting from the hypothesis that there is a crucial depth when the nail penetrates the battery where the ISC change from a local type to a more severe and larger short circuit. Fig 3.1_8 (a, b, c, d, e) shows the thermal behavior of the batteries with different penetration depth. The 6 mm depth trend is similar to that of 9 mm depth, for both of those tests the battery temperature rise rate is quite slow, they reached the peak value in about 600 s, with peak values of 47 °C and 63 °C respectively, greatly lower than that of the other tests. The temperature rise is due to the formation of a partial short circuit at the penetration position, the joule heat and exotherm reactions are generated in the local part of the short circuit, the heat generation is a bit larger than the heat dissipation, this leads to a slow rise of the temperature. The peak temperature is not high and after some time the energy is consumed by the short circuit itself, this leads to lesser heat generation and when the heat generation became lower than the heat dissipation the temperature dropped. The batteries from a macroscopic point of view showed leakage of the electrolyte due to the penetration but there was no open of the safety valve nor smoke generation, the batteries didn’t enter the Thermal Runaway state.

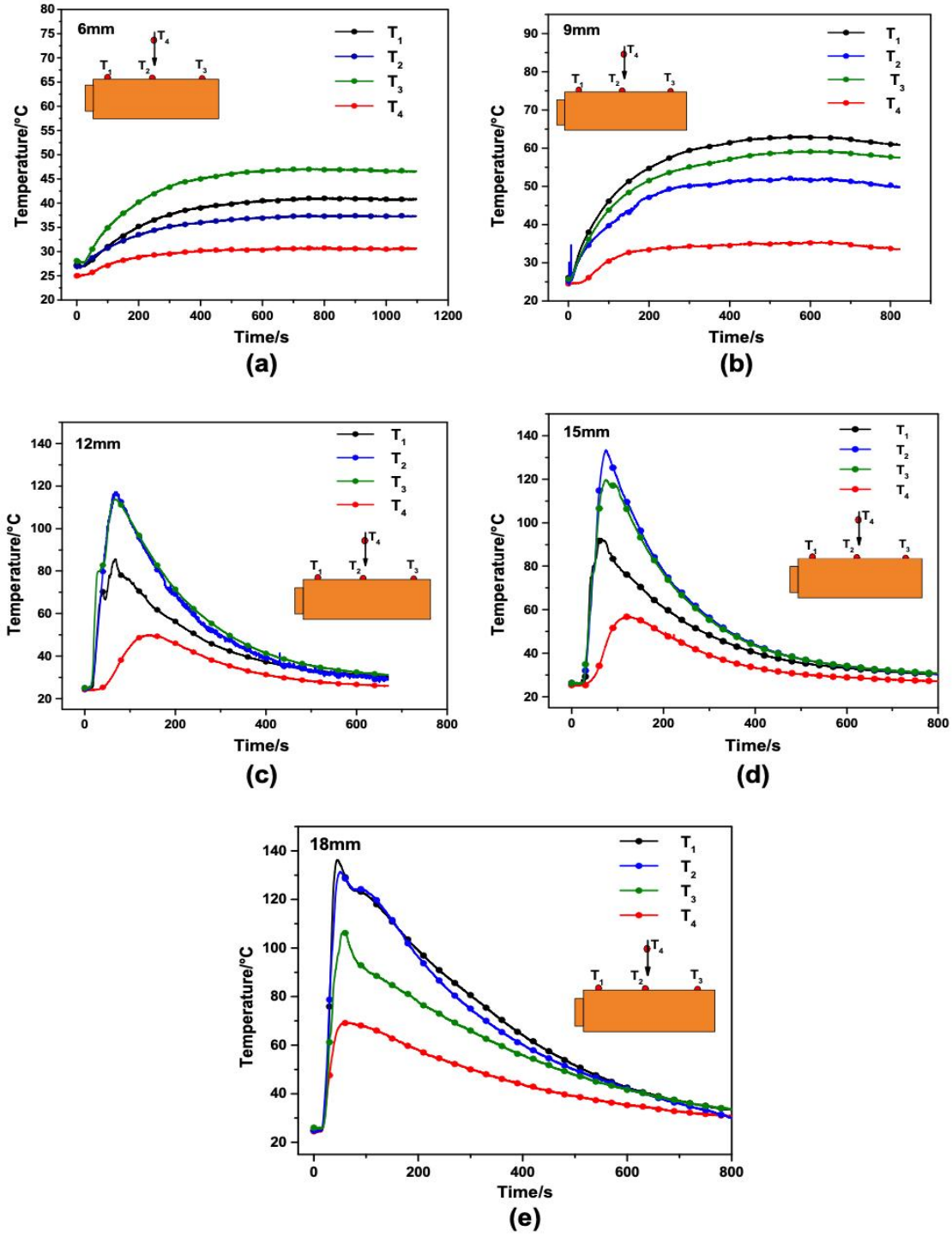


Fig.3.1_8

For penetration depth of 12, 15, 18 mm the thermal behavior totally changes. As can be seen from Fig.3.1_8 c, d and e the temperature rose quickly after the penetration, the peaks temperature are around 120 °C, significantly higher, and they reached the peak in about 50 s. all the

batteries experienced Thermal Runaway, the safety valve opened and released a great amount of white smoke. These finding support the hypothesis that when the battery is under a local ISC and/or the penetration depth is under a certain critical value, the battery does not experience thermal runaway. Another important aspect that has been found in this study regard the batteries' voltages; for 12, 15, 18 mm depth penetration the battery's voltage dropped from 3.4~3.5 V to 0.6 V rapidly after the penetration. The damage was so severe that it ended with the battery failure, the voltage reached the 0 V value. A different behavior is seen for the 6 and 9 mm tests as shown in Fig 3.3_9.

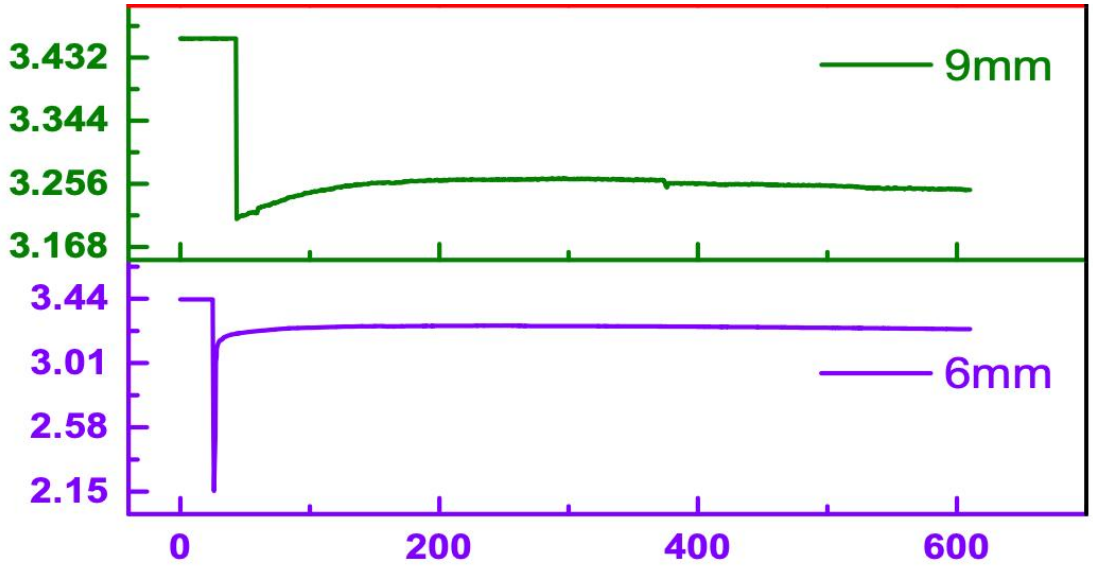


Fig 3.3_9

For the 9 mm depth the voltage dropped from 3.4 V to 3.1 V to then stabilize at 3.25 V. For the 6 mm depth the voltage dropped from 3.4 V to 2.15 V and the rose to 3.25 V. There are some reasons that explain the voltage recovery, first the ISC is a partial one which consume only a small amount of electrical energy. Second the electrochemical response of the battery is

triggered by the local heat generation and if the heat generation and rise rate are high enough then the local areas, the separator and the current collector can be melted. The melting of those components can cut off the current path to stop further discharge of the battery and ultimately the melting behavior determines if the voltages drops are recoverable or not. From this study can be said that a higher SOC leads to a more violent TR reaction, but even considering the safety issues we want to use batteries to the fullest of their capacity. The penetration speed does not greatly influence TR phenomenon, in an accident if the battery is pierced it just matters the fact that it's pierced, instead it matters at what depth arrived because penetration depth greatly in fluences TR phenomenon, after a certain critical depth value the ISC is large enough to trigger the Thermal Runaway. As can be seen from these studies the cause of TR is not just the occur of an Internal Short Circuit but the entity of the ISC itself, it must be large enough to lead to many internal chain reactions that lead to a totally uncontrollable behavior. ISC as presented for nail penetration test can be seen as a form of mechanical abuse but, as reported in the following chapters, others form of abuse lead to ISC and then to the untimely battery failure so even in stationary use, where mechanical incidents shouldn't happen, ISC can occurs. A large ISC is the main trigger for Thermal Runaway.

### *3.1.4 Thermal Abuse*

With the increasing of the temperature there can be electrochemical side reaction that can contribute to generate more heat, creating a self-feeding loop. If the temperature rise is local then the materials in that point can shrink or rupture, destroying the battery's structure itself causing TR phenomenon as seen for collisions in Mechanical Abuse. Localized high

temperature areas within a battery are usually bounded to its design; a poor design leads to high impedance at the metal contacts, to higher localized heat generation and uneven heat dissipation [24]. During transportation, storage and practical application LIBs are often stored in the form of modules, for stationary use they are stored as modules in fire-proof cabinets. If one of those batteries triggers Thermal Runaway phenomenon, then the adjacent batteries are affected by the nearby high temperature and that can be the trigger for the TR for all other batteries in the same module. This situation has been analyzed in [25]. The battery used was the 22 Ah with $LiFePO_4$ cathode and carbon based anode. The electrolyte was a solution of Lithium salt, $LiPF_6$, and a mixture of dimethyl, ethylene, methyl carbonate. The separator was in PP/PE/PP material. Battery's sizes were 100mm length, 20 mm width, 140mm height and nominal voltage was 3.2 V. In the study three different SOC have been used: 0%, 50% and 100%, the additional 75% has been used to better analyze the SOC impact on the Heat Release Rate (HRR). The battery was placed inside an oven, heated with a 550W heating plate which was tightly bounded to the cell's surface because, as foreseen, the battery case swelled during heating. The temperature's data were taken with five thermocouples placed as shown if Fig 3.1_10 The security valve expelled the accumulated gas generated by the high temperature, these gases were flammable and an external ignition source was used to ensure gas ignition and combustion.

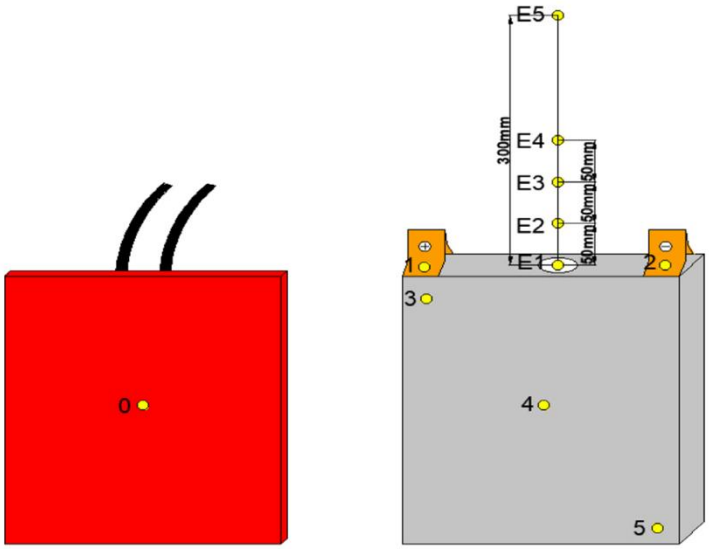

Fig 3.1_10

the thermocouples were placed in E1,2,3,4 each at 50mm from each other, while E5 was at 150mm from E4. It has been seen that TR phenomenon do not occur for 0% SOC due to low energy stored, as for 50% and 100% with trigger temperature of TR are 198.6°C and 184.8°C, respectively. The average temperature of voltage drop is 165.5°C which is higher than the melting point of the PE, 135°C, and pp, 165°C, separator. The separator melting does not cause an instantaneous drop of voltage but with its melting the electrodes are in contact with each other leading to an internal short circuit event, which cause undesirable exothermic reactions which further increase the battery heat generation and can potentially trigger the TR phenomena. Heath Release Rate is one of the most valuable tools to evaluate the fire hazard qualitatively, the total energy value of combustion and change to energy release with time can be obtained by the HRR profile and the combustion heat is calculated integrating the HRR curve. In Fig 3.3_11 are shown HRR plots versus time with different SOCs.

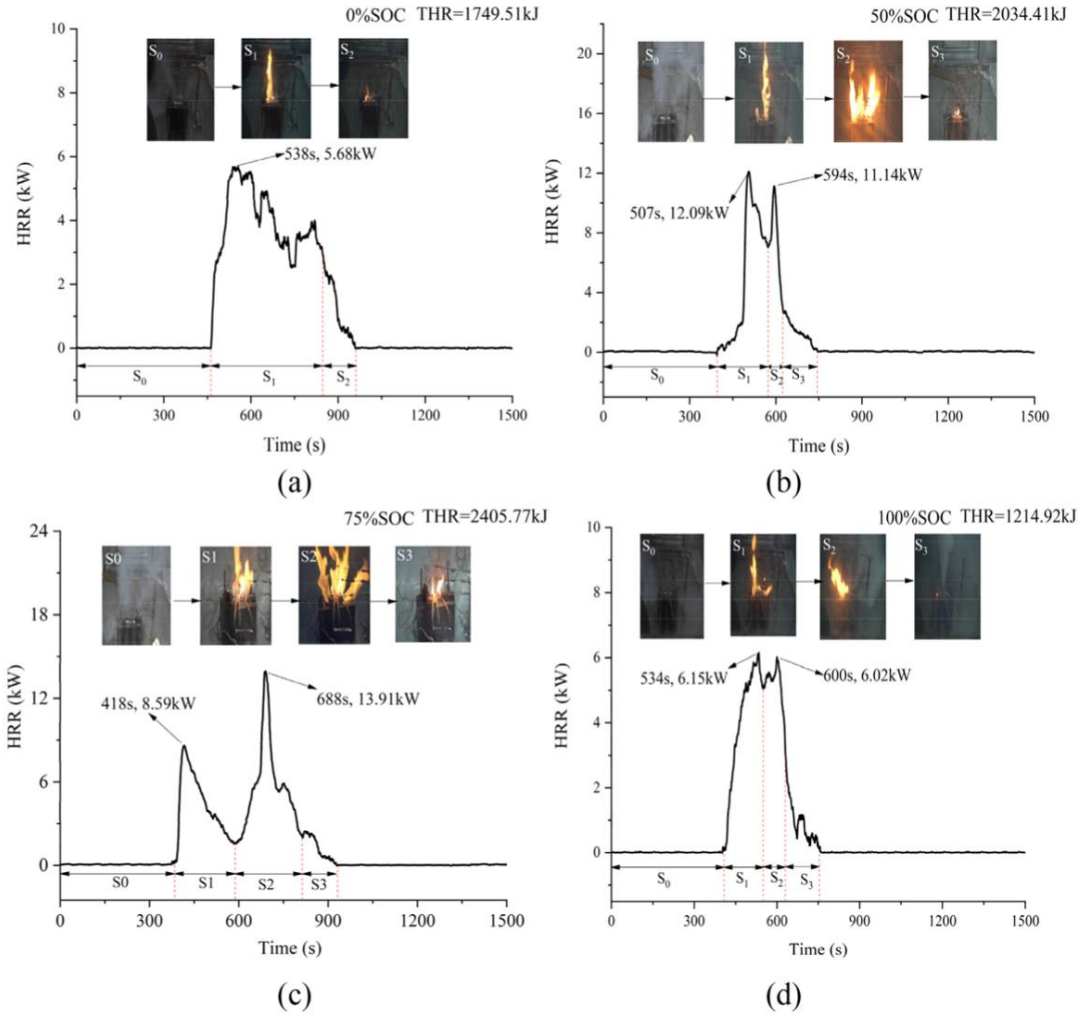


Fig 3.1_11

The pictures show the combustion stages. stage 1: venting, stage 2: combustion, stage 3: extinguishment.

The first HRR peak, for each state, is arising from the gas accumulated before combustion, in the venting stage, which can be influenced by the moment of ignition. The values of the second peak re corresponding to jet fire. The second peak of 0% SOC is much lower than the first because no jet fire occurs, as shown in the pictures. The 100% SOC values are lower than those of others SOC because of the more violent burning behavior, there has been a higher jet smoke production that obstructed the jet fire and the security valve on top of the battery burst and ejected a more powerful jet

flow which caused the extinguished of the jet fire, this led to an incomplete combustion of the cells. The 100% Soc may not have the highest heat of combustion but has the higher flammable gas generation and mass loss, it indicates that more combustible materials are ejected and may cause deflagration to release more heat. In the study it has also been found that also gas generation depends on the SOC. CO, which is a flammable and explosive gas, is generated by incomplete combustion and $CO_2$ and $LI_xC_6$ reduction and is higher for higher SOC, this is because:

- the lower SOC leads to a more stable and longer time combustion which results in more complete burning
- with higher SOC the combustible substances are ejected more violent which limit the oxygen consumption
- at higher SOC the $CO_2$ and $LI_xC_6$ can produce more CO

it has been also detected $H_2$ and HF generation, $H_2$ only in the 100% SOC case because of the incomplete combustion. HF, which is a corrosive gas, is also higher for the 100% SOC case because of the more violent combustion behavior that leads to a more electrolyte release and more reaction area with oxygen. This study shows that a local increase of temperature can cause damage to battery structure, prior to the combustion, leading to internal short-circuit and uncontrollable internal chain reaction. The local heat is not a direct trigger to TR phenomenon but can lead to other trigger's situations, if a nearby battery is on fire, then there is the risk of triggering all the others battery because of the presence of an ignition source. The analysis shows that the fire hazards are mainly governed by the thermal properties and the thermal properties can be characterized by the extreme

temperature and heat release. As safety measures for LFP lithium ions batteries the study advances the following proposals:

- considering the large amount of smoke production and no fire without and ignition source, is suggested a smoke detector instead of a heat detector
- different methods should be adopted for the various stages, for the stage 1 a chemical suppression method is suggested. Using suppressants to control the fire under tolerable levels. In the event of TR complete isolation is suggest to limit flying fire, which can be an ignition source for triggering other TR phenomena in the nearby batteries.
- After the flame is extinguished, the cell might pose potential threats such as deflagration and toxicity, adequate measures are recommended
- An adequate ventilation system, described in 3.1 is required, to prevent the formation of an explosive mixture and the removal of the toxic smoke produced which can pose lethal dangers

### *3.1.5 Electrical abuse*

A battery experiences electrical abuse when is in over-charging, over-discharging state or is undergoing an external short-circuit. They are analyzed separately in the following chapters.

#### *Over-charging*

There are many causes for over-charging, one is inconsistency of battery cells. Every single cell can enter independently in an over-charge state if it's

charged over the nominal voltage, the only form of prevention consists in a management system that can continuously monitors the voltage of every cell. Referring to a 40 Ah LIB containing $Li_yNi_{1/3}CO_{1/3}Mn_{1/3}O_2$(NMC) + $Li_yMn_2O_4$(LMO) composite cathode and a graphite anode, studied in [24] and [26], over-charge first cause electrolyte decomposition at the cathode interface, this reaction slowly increases the temperature and is followed by an excessive $Li^+$ deintercalation from the cathode. The cathode's material becomes unstable and start to release oxygen and the excess of $Li^+$ deposits on the anode to form Li dendrite. The heat and gas generation during these side reactions can lead to over-heating and subsequently, as seen, to irreversible damage of the internal structure of the battery. The over-charge process, as shown in Fig 3.1_12 and Fig 3.1_13 can be summarized in 4 different stages:

- Stage 1: the voltage increases steadily over the nominal cut-off voltage, in this stage there are no side reactions because of the large capacity of both the anode and the cathode. It's seen a little increase of battery's temperature and internal resistance.
- Stage 2: when the SOC exceed 1.2, side reactions occur inside the battery. At the cathode begin the dissolution of Mn ions in NMC + LMO composite cathode begins, meanwhile metallic lithium starts to deposit on the anode surface after the graphite anode is full of intercalated lithium. The deposited lithium reacts with solvent to thicken the SEI film, increasing the internal resistance. Temperature start rising due to joule heat and side reactions.
- Stage 3: the oxidation of electrolyte increases as the cathode potential increase. A large amount of heat and gas is generated, the battery casing starts to swell. SEI decomposition happens at high temperature. As shown in fig 3.1_12 the voltage slight drop after a peak at 5.2V.

- Stage 4: the SEI film ruptures, ruptures the internal structure of the battery, directly connecting the electrodes leading to internal short-circuit. The internal energy of the battery is released instantaneously triggering the TR phenomenon and at peak temperature of 780°C.

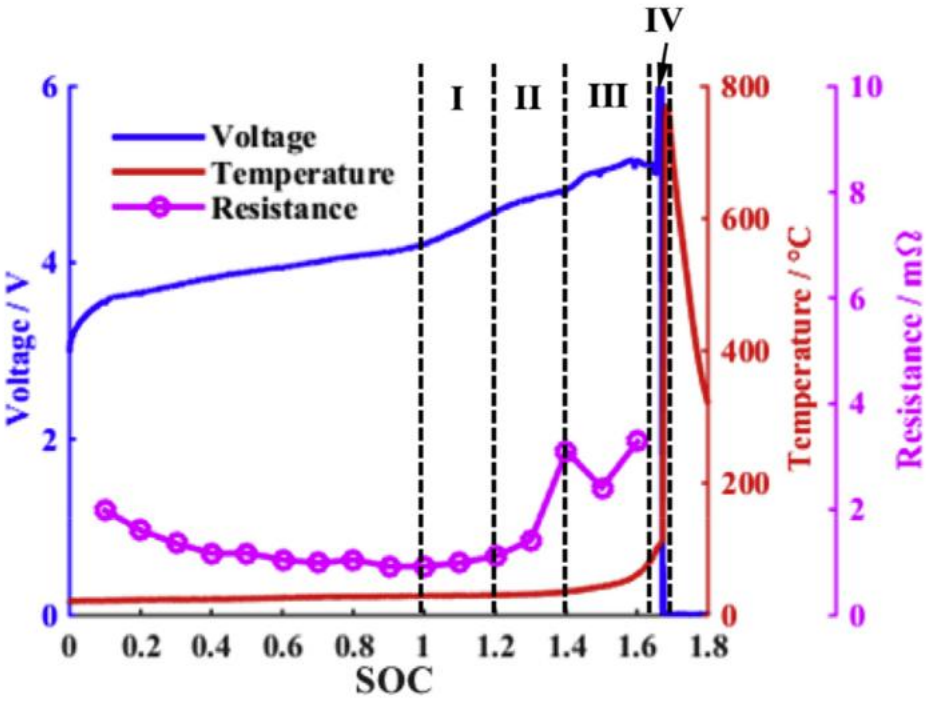


Fig 3.1_12

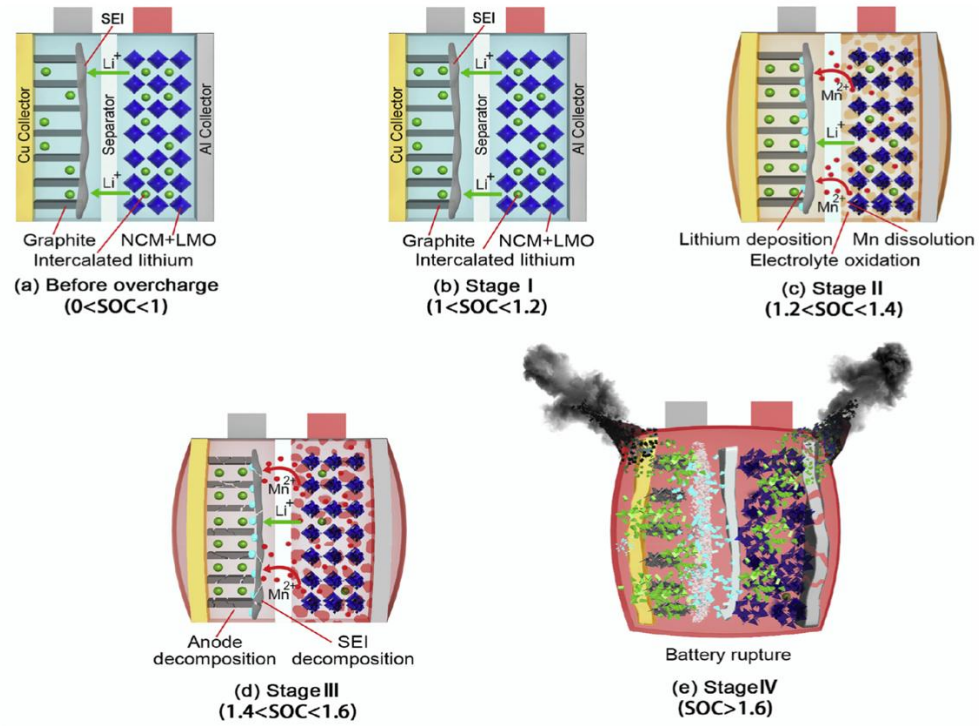

Fig 3.1_13

In the study [27] the over-charging behavior of three kinds of $LiFePO_4/C$ with 25 Ah, 60 Ah and 200 Ah, is analyzed, with a rated voltage of 3.2 V for all batteries. This study identifies 3 stages of the over-charging behavior, they are shown in Fig 3.1_14

- Stage a: this stage identifies a slowly increase of temperature from room temperature for 25 Ah and 60 Ah batteries, the rise rate increases after 70°C and 86.6°C respectively, for the 200 Ah battery a gradual increase of temperature is seen. Temperature-time behavior for the three batteries is shown in fig.5.
- Stage b: is TR phase, all battery temperatures rise quickly. The starting and highest temperatures are respectively 120°C and 263°C for 25 Ah, 131°C and 14°C for 60 Ah, 116°C and 313°C for 200 Ah. It's seen that battery's highest temperature has nothing to do with battery's capacity.
- Stage c: this is the cooling stage, after reaching the highest temperature due to TR the battery temperature starts to decrease very rapidly because of the extinguishment of the phenomenon. In Fig.5a the battery temperature after 40 min drops because the thermocouples fell during the test.

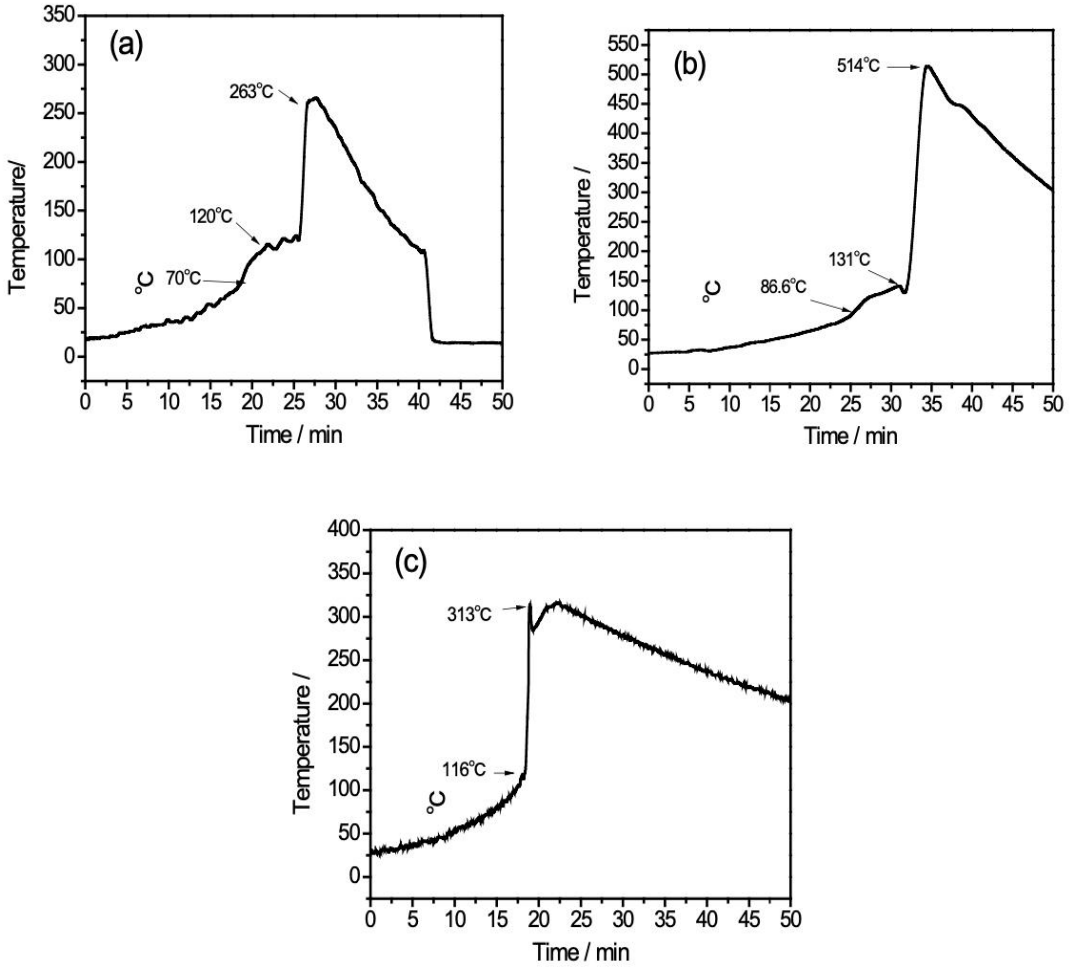


Fig 3.1_14

One of the hypotheses of the cause of lower highest temperature of 200 Ah battery respect to the 60 Ah one, is that the 200 Ah has significantly larger surface than the other, so it has a better heat dissipation and lower heat accumulation inside the battery. Apart from that, the 200 Ah battery is the first one to experience Thermal Runaway and its temperature rise rate is the highest, probably because it has the largest capacity and the largest scale of side reactions.

### *Over-Discharging*

The process of over-discharge is very similar to the over-charge, some cells reach the SOD (State Of Discharge) faster than others thus, an over-discharge process takes place if a one of those cells if further discharged. For $LiCoO_2$/C Lithium-ion batteries, forced over-discharge continuously generates $Li^+$ from the anode which change the graphite structure and damage the SEI. At the very deep of SOD there can be the oxidation of a copper current collector accompanied with the potentially deposition of released copper ions on the cathode surface and too much copper deposition results in short-circuit of the cell. SEI dissolution is the main reason for battery degradation and dissatisfactory cycling performance [24].

### *External Short-Circuit*

An external short-circuit occurs when cathode and anode of the same cell are in direct contact through a conductor. In this case $Li^+$ and electrons migrations happen simultaneously causing a rapidly discharge of the battery releasing the heat relatively evenly and quickly. It's seen an increase of internal temperature and a cell rupture causing electrolyte leakage as reported in [24]. Hao et al. studied the behavior of Lithium-Ion batteries under external short-circuit fault, and variation of life cycle and internal resistance [28]. In the experiment they used a battery 18650 type whose dimensions are: 65mm height and 18.9mm diameter (cylindrical battery) with a rated capacity of 2600 mAh. Positive electrode $LiCoO_2$, negative electrode was in graphite and the electrolyte was ethylene carbonate, diethyl carbonate and lithium hexafluorophosphate ($LiPF_6$). The behavior o

f a single battery under external short-circuit is shown in Fig 3.1_15. Copper was used to trigger the external short-circuit because its resistance, of 4.39 mΩ, was smaller than the battery's internal resistance.

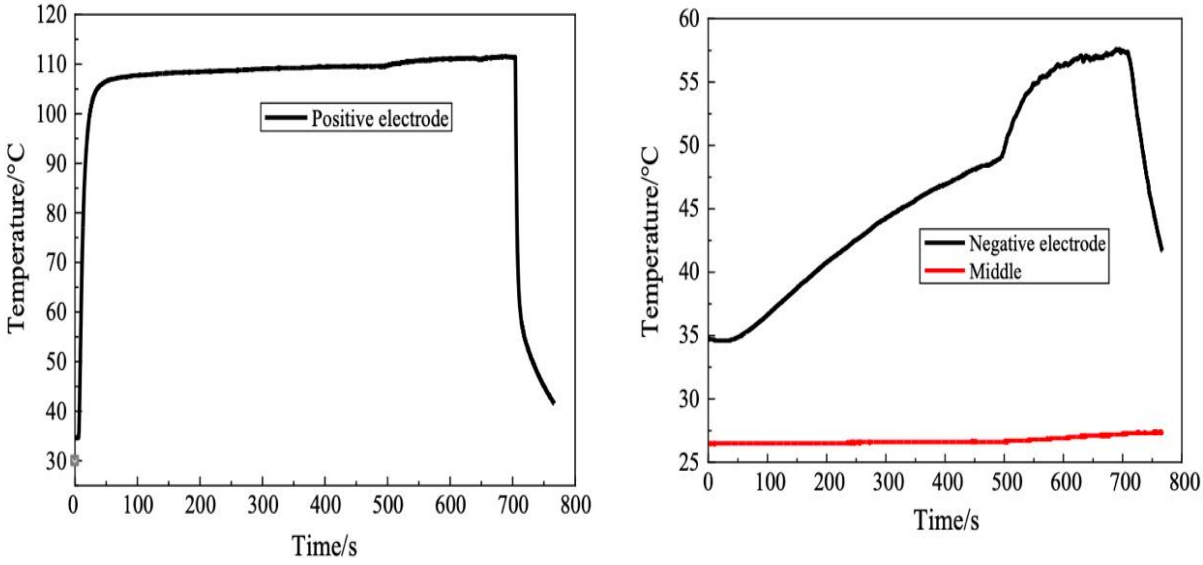


Fig 3.1_15

As shown, temperature of positive electrode rose to 110°C after the short-circuit started then, due to the intervention of some safety device, PTC (positive temperature coefficient) and CID (current interrupt device), the temperature entered a stable period. Due to heat accumulation, there can be side reaction of the electrolyte with positive and negative materials, causing the temperature to rise until the rise rate gradually decrease with the continuous electrolyte consumption until the final battery failure. After the study of a single battery there have been studies on modules behavior. Two different 3 batteries modules connections have been analyzed, as shown in Fig 3.1_16, two series and one parallel (2S*1P) and two parallel and one series (2P*1S).

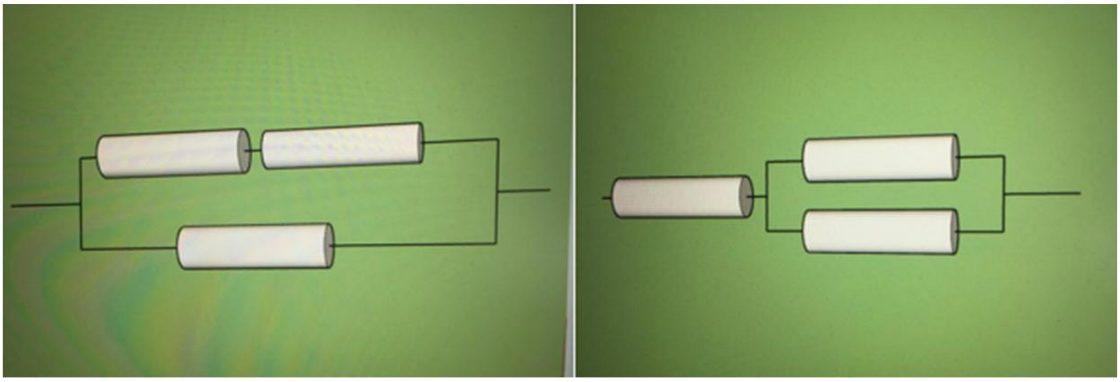

Fig 3.1_16

In Fig 3.1_17 a and b are shown the behavior of the two modules connection, respectively 2S*1P and 2P*1S. For the 2S*1P the battery experienced three short-circuit events, in the first the positive electrode temperature rose to 110°C and then the circuit disconnects the battery and the temperature drops. After that the battery entered the second short-circuit event and the temperature rose to 120°C, it was disconnected again and then entered the third short-circuit event where the temperature stabilized at 110°C. The temperature trend of the battery middle follows the positive electrode trend but with the environmental heat dissipation the temperature rise rate was far more less than the positive electrode rise rate. Fig.8b shows the thermal behavior of the 2P*1S module, it can be seen that when the first short-circuit occurs the temperature rose to 110°C in about 100s, then the circuit was disconnected and the battery's temperature dropped. After 100s the circuit was turned on again to make the battery short-circuited, the temperature rose to 120°C probably due to side reaction in the electrolyte decomposition, then it has been disconnected again. When the battery was short-circuited for the third time, due to the electrolyte consumption in the previous short-circuit, the maximum temperature for positive electrode has been 110°C, while the

temperature in the middle of the battery rose to 60°C. The figure shows that when the battery was disconnected for the first time the temperature continued to rise because the heat conduction was greater than the heat dissipation. This also happened during the second disconnection, the anode and middle point temperatures continued to rise slowly, until the heat dissipation became greater than the heat conduction, then the middle temperature begun to decrease.

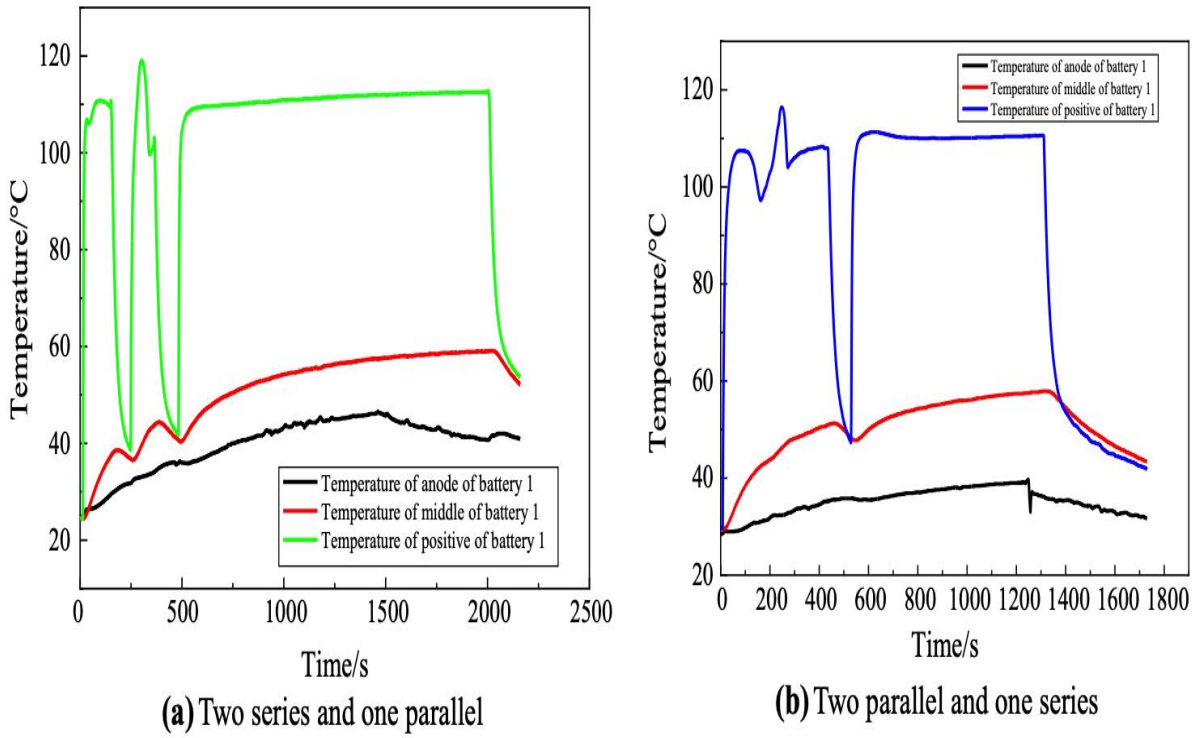


Fig 3.1_17 a and b

After the three batteries module a nine batteries module external short-circuit was conducted. The tests have been done with a 3P*3S configuration and under different SOC, 100%, 90%, 80%. Fig 3.1_18 shows the thermal behavior of respectively 100%, 90, 80%, SOC.

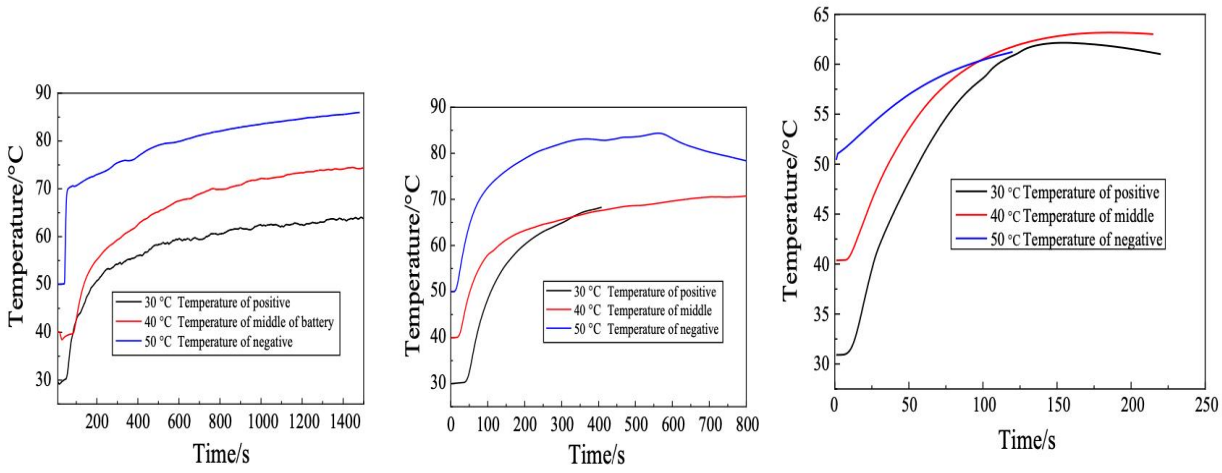


Fig 3.1_18

When the external short-circuit occurred it's seen that in the 100% SOC case the temperature rose immediately to 70°C and then it increased gradually with time. In the 90% case the temperature rose higher than the 100% case but with a much gentler trend compared to the previous case. In the 80% case the temperature rise rate is significantly lower than those of the other cases. After calculation, it can be seen than the maximum temperature rise rate decreases with the decrease of the SOC. After the external short-circuit experiments, cycling charge and discharge experiments at different temperatures were conducted to analyze change of capacity and internal resistance of the batteries. The remaining capacity is the most effective quantity representing the performance of the battery, when the capacity decreased to 80% the battery would be scrapped. Fig 3.1_19 is a schematic diagram of the change of the remaining battery capacity with the number of cycles at an ambient temperature of 30°C.

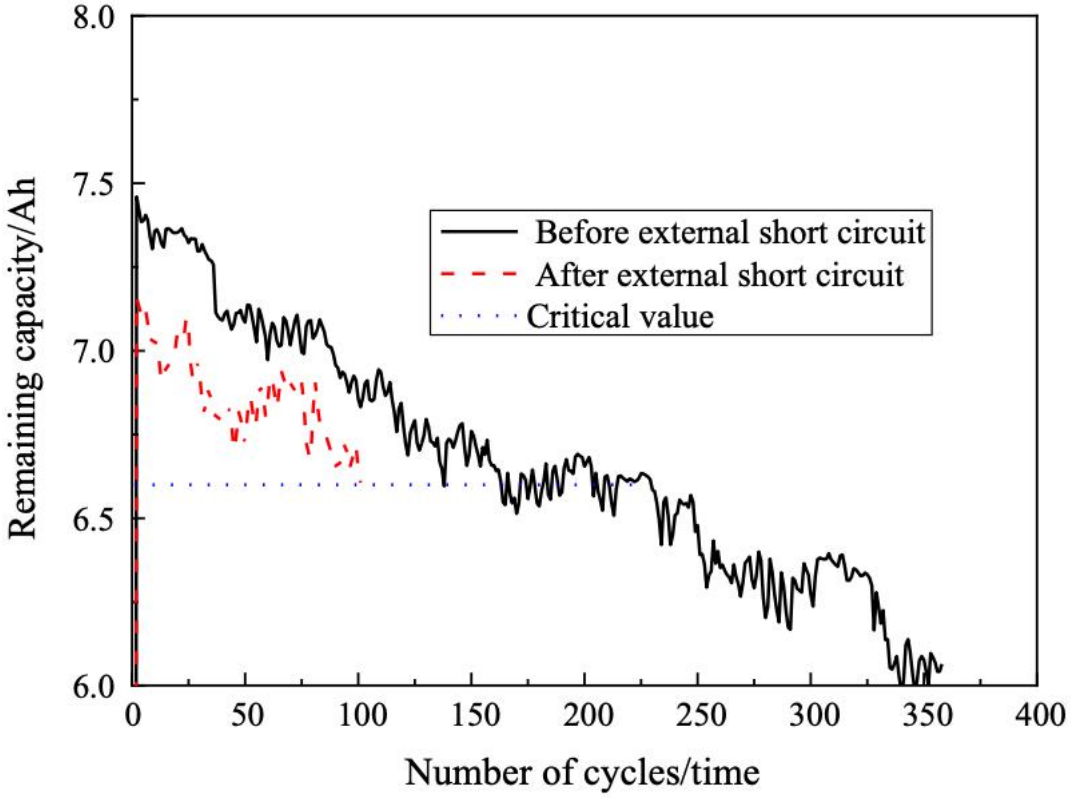


Fig 3.1_19

In normal conditions the battery reaches the 80% failure threshold at around 200 cycles, after the external short-circuit event the limit lowered to 100 cycles. The tests have been done even under an ambient temperature of 40°C and 50°C and it's seen that the threshold values are 250 cycles and 160 cycles in normal condition and 105 and 100 cycles after the fault respectively. The battery works better at 40°C but for every ambient temperature the life cycle is significantly reduced after the fault. Internal resistance is another parameter that represent the battery performances, even these tests have been done under different ambient temperature: 30°C, 40°C and 50°C; under all these different conditions the battery always shown the same behavior, the new battery at the beginning had a high internal resistance, of about 320 mΩ, due to the fact that the SEI

film forms gradually during the initial cycle and then the internal resistance greatly reduces. Starting from a value of 80 mΩ, the internal resistance grew up to 200 mΩ after 350 cycles, this increment is due the conductivity of electrolyte and ions migration ability decrease as the number of cycles increase, the battery deteriorates. Fig 3.1_20 shows the internal resistance trend at an ambient temperature of 30°C, the trend in black (the one before the external short-circuit) is fundamentally the same for 40 and 50°C.

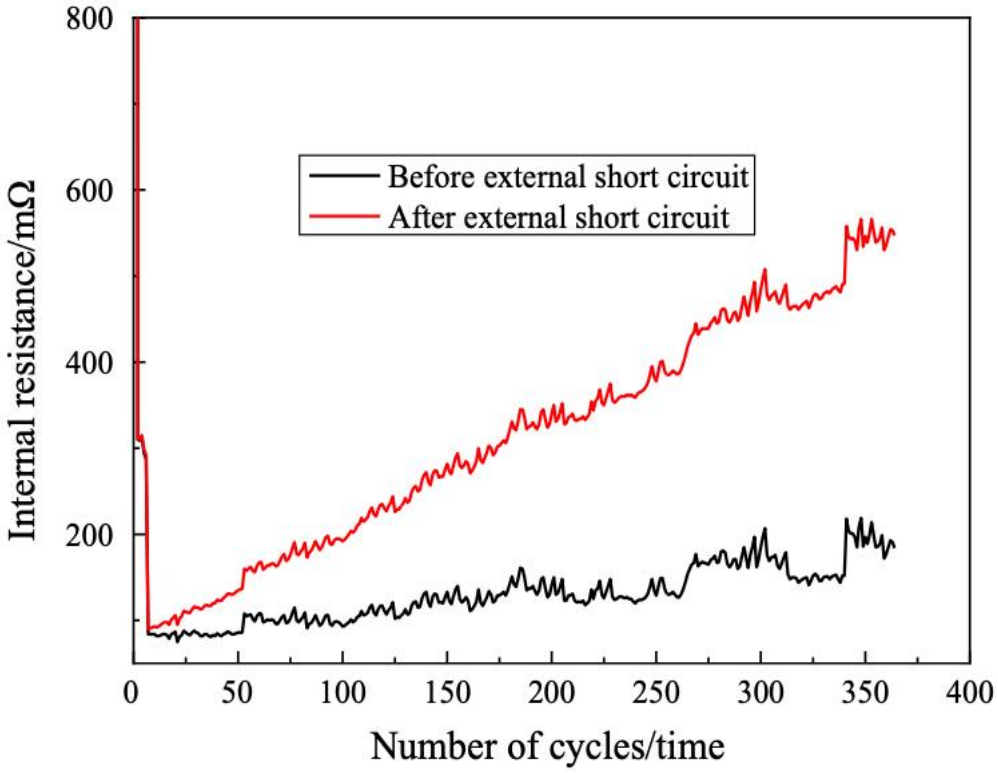


Fig 3.1_20

In Fig 3.1_20 at 30°C, it's seen that after an external short-circuit the rate of increase of internal resistance is much higher than the rate under nor al conditions, this is because under an external short-circuit the impact force od temperature and pressure on the SEI film became strong, causing the rupture of the SEI itself and contact between carbon negative electrode and

electrolyte at the rupture point. Then the film resumed on the surface on the carbon negative electrode and repeated film formation led to thickening of the SEI film, increasing the internal resistance. This study shows that an external short-circuit severely impact the operative life of a Lithium Ions battery, greatly reduces the number of cycles and increases the internal resistance diminishing the battery's performances. It's surely an event that must be avoided and taken precautions against, but its effects are not so irreversible and hazardous as the TR phenomenon. As stated in the study PTC and CID measures shall be provided as well as thermal sensor to identify an abnormal battery's behavior.

### *3.2 GASES GENERATION*

Zhang et al. [23] studied the gases composition of emissions of Lithium Ions Batteries under Thermal Runaway Phenomenon. The batteries analyzed were 18650 type, with positive electrode in li$CoO_2$ and the negative one in intercalated graphite. The electrolyte had an organic solvent that included DMC (Dimethyl Carbonate) and EMC (Ethyl Dimethyl Carbonate), the separator consists of PE (polyethylene) and PP (polypropylene), the lithium salt in the electrolyte was $LiPF_6$. The Thermal Runaway process was triggered by a heating device and the behavior, on time, can be divided in three stages according to Fig 3.2_1. There are two points where the temperature/time trend changes its behavior, the first is at the rupture time of the safety valve, as a safety measure, and the peak temperature of the whole process. In stage 1, before the opening of the safety valve, there are no analyzed gas obviously since the valve was still close. In stage 2 the safety valve opened and then it was possible to analyze the gases emitted,

the decomposition of $LiPF_6$ electrolyte generated $PF_3$, $C_2H_4$ and $CO_2$ at the same time. Three free radicals H, $CH_3$ and $C_2H_5$ are generated with $Li^+$ through reduction reaction during the decomposition process of electrolyte organic solvent. These radicals are supposed to be the cause of the formation of flammable hydrocarbons with length of 3-8 carbon chains during Thermal Runaway and the hydrocarbons production causes the thick milky smoke ejection and combustion that characterized the Thermal Runaway state. The instant of Thermal Runaway onset ($TR_{onset}$) was defined as the time at which the temperature rise rate was greater than 1 °C/s and that lasted more than 3 s.

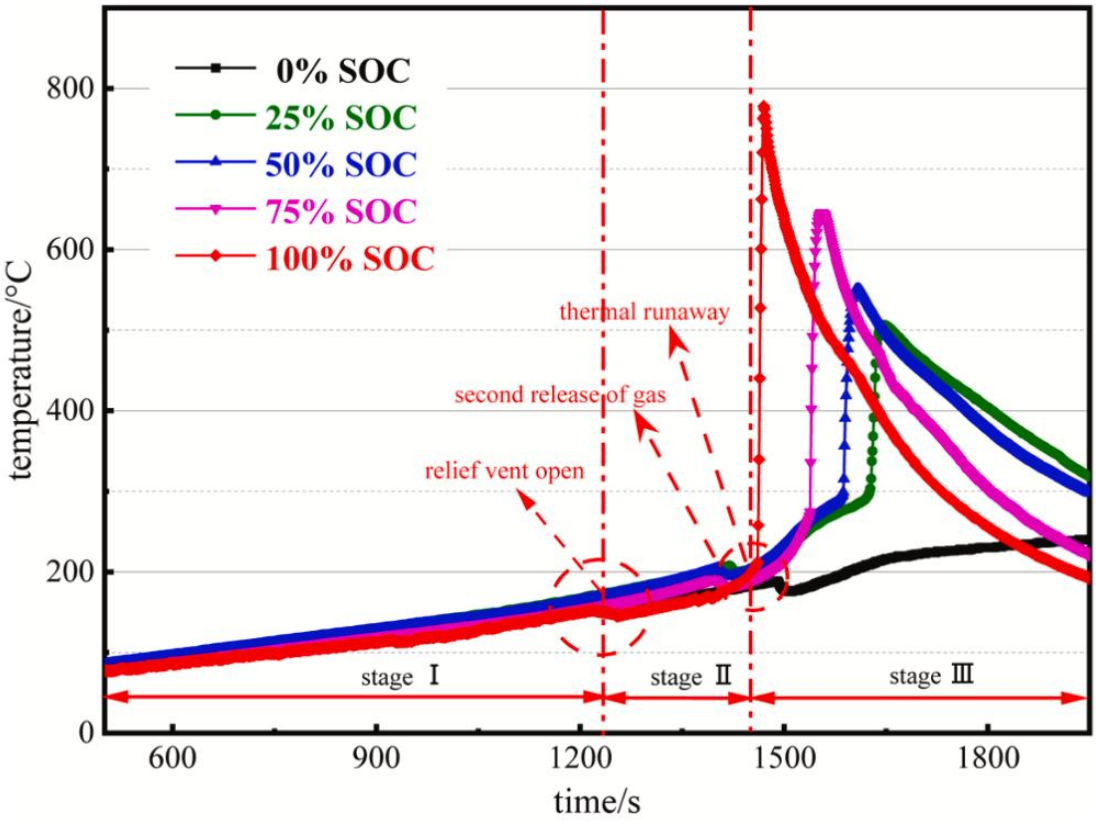


Fig 3.2_1

Fig 3.2_1 shows the thermal behavior of batteries with different SOC, with the increasing of the charge it's seen that also increase the highest

temperature while decrease both the Thermal Runaway Temperature and Time onset. Higher the SOC leads to a more violent behavior; the safety significantly decreases. The onset values are reported in the following table.

| SOC (%) | Safety valve opening T (°C) | $TR_{onset}$ time (s) | $TR_{onset}$ temperature (°C) | Highest temperature (°C) |
|---|---|---|---|---|
| 0 | 189.2 | - | - | 277.8 |
| 25 | 207.9 | 1627 | 303.5 | 506.6 |
| 50 | 204.5 | 1588 | 299.2 | 550.8 |
| 75 | 191 | 1537 | 269.1 | 645.5 |
| 100 | 152.4 | 1462 | 212.1 | 777.7 |

Table 3.2_1

The maximum temperature of the 0% SOC is only 277.8 °C, the Thermal Runaway did not even occur.

The gases analysis shows that the components of exhausted gas tend to increase with the increasing of the SOC, this is related to the fact that some side reactions generated by gas components need to reach a certain temperature to happen. According to the study, the concentration of 2-6 carbon chain length hydrocarbons increases with the increase of SOC leading to a more severe Thermal Runaway behavior such as combustion and jet fire. The following figure Fig 3.2_2 shows that the unsaturated hydrocarbon increases with the SOC while the alkanes show the opposite behavior. The $C_2H$ content in the 100% SOC is six times greater of the 50% SOC batteries, while the $C_4H_{10}$ content is one third of that of the 50% SOC batteries.

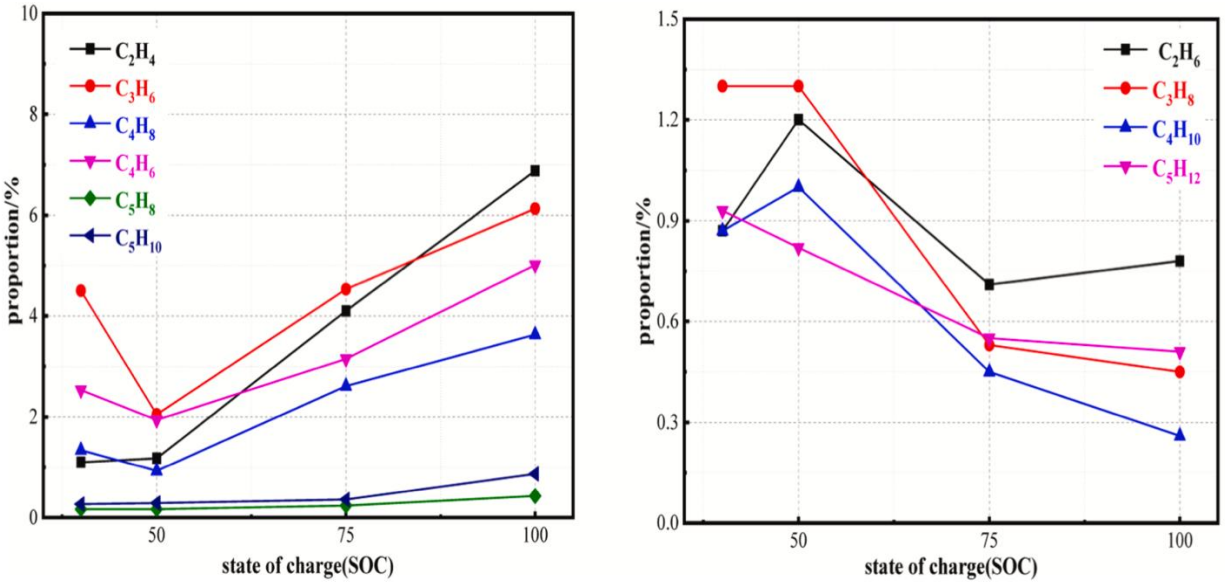


Fig 3.2_2

In table 3.2_2 are listed all the gases that have been found out in this study and in which group of SOC have been found.

| Exhausted component | 0% SOC | 25% SOC | 50% SOC | 75% SOC | 100% SOC |
|---|---|---|---|---|---|
| CO | x | x | x | x | x |
| $CO_2$ | x | x | x | x | x |
| $PF_3$ | - | x | x | x | x |
| $C_2H_4$ | - | x | x | x | x |
| $C_2H_6$ | - | x | x | x | x |
| $C_3H_6$ | - | x | x | x | x |
| $C_3H_8$ | - | x | x | x | x |
| $C_3H_4$ | - | - | - | - | x |
| $C_2H_4O$ | - | x | - | x | x |
| $C_4H_8$ (cis-2-butene) | - | x | x | x | x |
| $C_4H_8$ (trans-2-butene) | - | x | - | x | x |

| | | | | | |
|---|---|---|---|---|---|
| $C_4H_6$ | - | x | x | x | x |
| $C_4H_{10}$ | - | x | x | x | x |
| $C_4H_8$ (isobutylene) | - | x | - | x | x |
| $C_5H_{10}$ (Dimethyl ethylene) | - | x | x | x | x |
| $C_5H_{10}$ (N-pentene) | - | x | x | x | x |
| $C_5H_{12}$ | - | x | x | x | x |
| $C_4H_8O$ | - | x | x | x | x |
| $C_3H_6O_3$ | x | x | x | x | x |
| $C_6H_{10}$ | - | - | - | x | x |
| $C_6H_{12}$ (Methylcyclopentane) | - | x | - | x | x |
| $C_6H_{12}$ (1-hexene) | - | x | x | x | x |
| $C_6H_6$ | - | x | x | x | x |
| $C_6H_8$ | - | - | - | - | x |
| $C_4H_8O_3$ | x | x | x | x | x |
| C7 hydrocarbon | - | x | x | x | x |
| $C_7H_8$ | - | x | x | x | x |
| C8 hydrocarbon | - | x | x | x | x |
| $C_8H_{10}$ | - | - | - | - | x |
| $C_8H_8$ | - | x | x | x | x |

Table 3.2_2

The study also tries to identify for every SOC a general LEL and UEL of all exhausted gas. the values are reported in the following table 3.2_3. Since the 0% SOC group of batteries did not experienced TR there is no need to identify these hazardous levels.

| SOC % | LEL % | UEL % |
|---|---|---|
| 25 | 7.25 | 47.95 |
| 50 | 10.98 | 40.06 |
| 75 | 6.53 | 51.82 |
| 100 | 3.97 | 61.35 |

Table 3.2_3

As expected the LEL, apart for the initial rise, tend to decrease with the SOC, while the UEL is related to the intensity of the thermal runaway reactions; at low SOC the electrolyte can fully react, due to a quieter behavior, in the air to produce a large amount of $CO_2$, while the CO and other combustible hydrocarbons content is lesser than that of higher SOC, which make the gas similar to an inert gas and then shows a narrow explosion limit range. The gaseous emissions during a Thermal Runaway phenomenon show the presence of toxic, cancerous and explosive substance, hence an adequate ventilation is required in the battery housing as presented in the previous chapters and for enchanting the housing safety form this study can be seen that the 50% SOC value can be the safer as the exhausted gas combustion explosive danger is the lowest. The LEL and UEL value should be choose in accordance with the appropriate standard.

## *3.3 Li-Ions batteries standards tests*

The most common Lithium-ions battery is the one with the in $LiFePO_4$ cathode and, as said in the previous chapters, it's the safer as said from the studies proposed in this work. $LiFePO_4$ has an ordered olive structure and strong P-O covalent bonding forming a three-dimensional structure with

excellent thermodynamic and kinetic stability. $LiFePO_4$ has also low reactivity with ordinary organic electrolyte, so cathode containing it have good cyclability [24]. The separator, whose role is to physically separate the cathode from the anode but guarantying the ions transfer, are normally polyolefin based porous membranes, which are thermically unstable and mechanically fragile. They shrink at elevate temperature causing battery failure to ISC. Current studies show positive progress in separator research, new separator materials and structures which can work normally at high temperature have been developed and separators coated in ceramic particles start to undergo degradation at about 250 °C. The electrolytes used are usually liquid-organic carbon based and they can combust or even explode when exposed to air due to their extreme flammability, adding fire-retarding materials or materials that can enhance thermal stability could lower the fire and explosion risks of Lithium Ions batteries. External measures that can enhance the safety level are cooling system, ventilation requirements must be meet to prevent the formation of an explosive mixture when gases are released from a battery, and there can be air cooling system, both natural or forced ventilation, and liquid cooling system which are more efficient but exist the possibility of the instauration of an external short circuit and/or electrochemical corrosion due to the fact that the battery has to be immersed in the cooling liquid. It is the most efficient and convenient measure but due to the previous doubts, this system is not implemented in on board EVs batteries, it can be a wise alternative for stationary use. To enhance the cooling effect, for any cooling system, optimization of inner cells distance in the battery is recommended but the battery must still be efficient and bigger channels for cooling system create uneven temperature distribution. Ideally the channel size shall match the

coolant's Reynolds number. Fig3.3_1 shows the effect of a working cooling system and the uneven temperature distribution inside the channels.

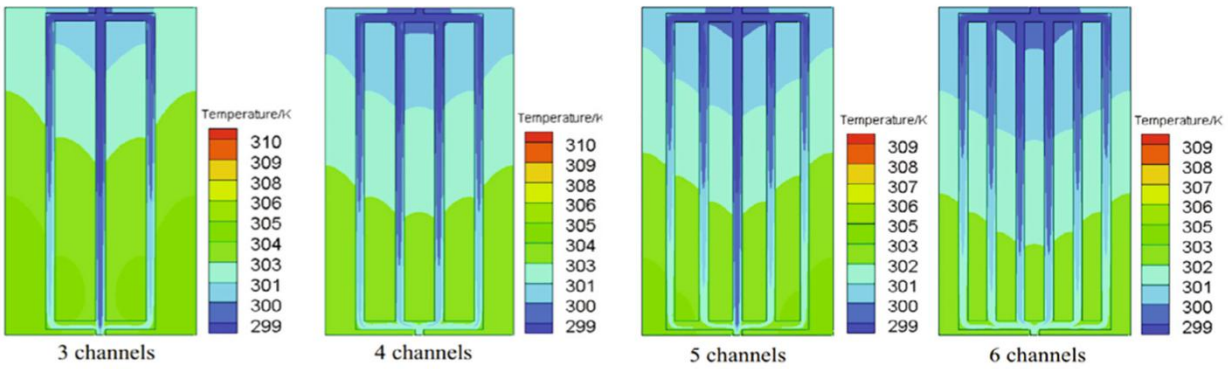


Fig 3.3_1

As the battery power density increases its fundamental to increase the heat transfer coefficient since, as said in the previous chapters, the TR behavior gets more violent and severe with the increasing of the SOC and power. Even a single cell failure can be enough to cause severe damages to adjacent cells ending with the battery failure, which can be cause for the failure of nearby batteries. To avoid this possibility control on every cell and a balancing power system are suggested. Balancing the cells can be done passively using the joule effect to dissipate the excess energy that a cell can have respect to others, or actively with a monitoring system which can control every cell to discharge the only overcharged one and putting the others to stop until power equalization is over. It's also possible to have an active system which can directly use the more charged cell to charge the others instead of dissipating the excess energy. Since TR phenomenon is the main cause of accidents for Lithium Ions batteries the batteries must surpass safety testing standard before being mass produced. The testing

standards and procedures are different from country to country as everyone has its own:

- Chinese standard GB/T 31,485
- Society Automotive Engineers (SAE) standard 2464
- IEC standard IEC62133
- United Nation standard UN38.3
- Japanese Industrial standard (JIS) C8714
- Underwriters Laboratories (UL) standard UL2580
- International Standard Organization (ISO) standard 16750-2

In the following table are presented the testing standard specifications of different tests and standards. The tests are heating, over-charge, over-discharge, short circuit and nail penetration, while the standards proposed are GB, SAE, IEC, UL, VW (Volkswagen) and GM (general motors).

| | GB/T31485 | IEC62133 | UL2580 | SAE J2464 | VW PV8450 | USABC-GM |
|---|---|---|---|---|---|---|
| HEATING | Heating at 5°C/min form 25°C to 130°, hold for 30 mins | 130°C, 10 mins | 150°C, 60 mins | Max, stable temperature | 2°C/ min to 130°C or 200°C, hold for 30 mins | 0.5°C/ mins, to 50°C-150°C hold 30 mins |

| | | | | | | |
|---|---|---|---|---|---|---|
| EXTERNAL SHORT CIRCUIT | For 10 mins, R≤5mΩ | 80±20mΩ | R≤5mΩ Till fire, explosion or no temperature change | R≤5mΩ for hard short R≥5mΩ For soft short | Short for 10 mins R≤1mΩ R=5mΩ R=10mΩ | Short for 10 mins, R≤5mΩ |
| OVER CHARGE | 100% SOC overcharge to $1.5V_{max}$, or charge for 1 hour at 1C | Overcharge to 250% SOC at 1C | Overcharge at 200% SOC at 1C | Overcharge at 200% SOC at 1C | Overcharge to $1.1V_{max}$ or 5mins at 1C | Overcharge the 100% SOC ell at 1C for 1 hour or $1.5V_{max}$ or venting |
| OVER DISCHARGE | Over-discharge the 100% SOC cell at 1.5C for 1 hour | Over-discharge the 0% cell at 1C for 90mins | Over-discharge the 0% cell at 1C for 90mins | Over-discharge the cell to- 100% SOC | / | Over-discharge the 100%SOC cell until venting |
| NAIL PENETRATION | Penetration rate 25mm/s, 100% depth, nail diameter 5-8mm | / | 80mm/s, diameter 3mm, 100% depth penetration | 80mm/s, diameter 3mm, 100% depth penetration | 0.1 mm/s, diameter 1mm, 2mm depth | 80mm/s, diameter 3mm, 100%depth |

Table 3.3_1

It's clear that in the absence of a unified and common regulation every standards agency has the liberty to determine the tests in which way it find more appropriate. Successfully passing these safety tests does not guarantee a battery's safety in real life performance conditions, especially for battery installed onboard of EVs, the European Council for Automotive (EUCAR) and the SAE classifies the batteries on the results of the safety tests. They identified seven hazard levels:

| HAZARD LEVEL | DESCRIPTION | CLASSIFICATION CRITERIA AND EFFECTS |
|---|---|---|
| 0 | No effect | No effect, no loss of functionality |
| 1 | passive protection activated | No damage or hazard, reversible loss of function. Replacement or resetting of protection device is sufficient to restore normal functionality |
| 2 | Defect and/or damage | No leakage, no venting, no flame, no rupture, no explosion, no TR. Irreversible loss of function due to damage, necessity of repair |

| | | |
|---|---|---|
| 3 | Minor leakage /venting | Evidence of cell leakage or venting, total weight loss <50% electrolyte total weight |
| 4 | Major leakage/venting | Evidence of cell leaking or venting, total weight loss >50% electrolyte total weight |
| 5 | Rupture | No explosion nut rupture of the mechanical integrity of the container, resulting is release of the content. Even flying parts of active mass but the kinetic energy is not high enough to damage the surrounding |
| 6 | Fire or flame | Ignition and sustained combustion of flammable gas or liquid for at least more than 1 s. sparks are not flames |

| | | |
|---|---|---|
| 7 | Explosion | Completely disintegration of the cell. The kinetic energy released is sufficient to cause pressure waves and projectiles that can cause structural damage and pose severe threat to person's safety. Hazard for the environment due to the high energy released, gases release, high temperature and flames |

Table 3.3_2

Particular attention must be paid for the housing room/container of the batteries, anti-fire- and fire-resistant closet exist and are produced especially for Lithium Ions batteries of stationary use [24]. The chosen room/closet must be fire resistant to contain and lower the fire propagation from a battery under TR to the nearby batteries and other housing closets. They also must be provided with an adequate ventilation system to disperse the many dangerous gases that are released during TR that can directly endanger personnel's safety, for its toxicity or corrosiveness, and dissolve possible explosive mixture.

# 4 Experimental Campain and Laboratory Circuitry Description

The laboratory test circuitry has been used to determinate charge and discharge performances of the battery tested with a particular attention on the thermal behavior. The circuitry had to measure voltages, currents, on spot temperature and to make a circuit that can be used for both charge and discharge a linear power supplier has been used. The laboratory Circuitry is shown in Fig 4_1.

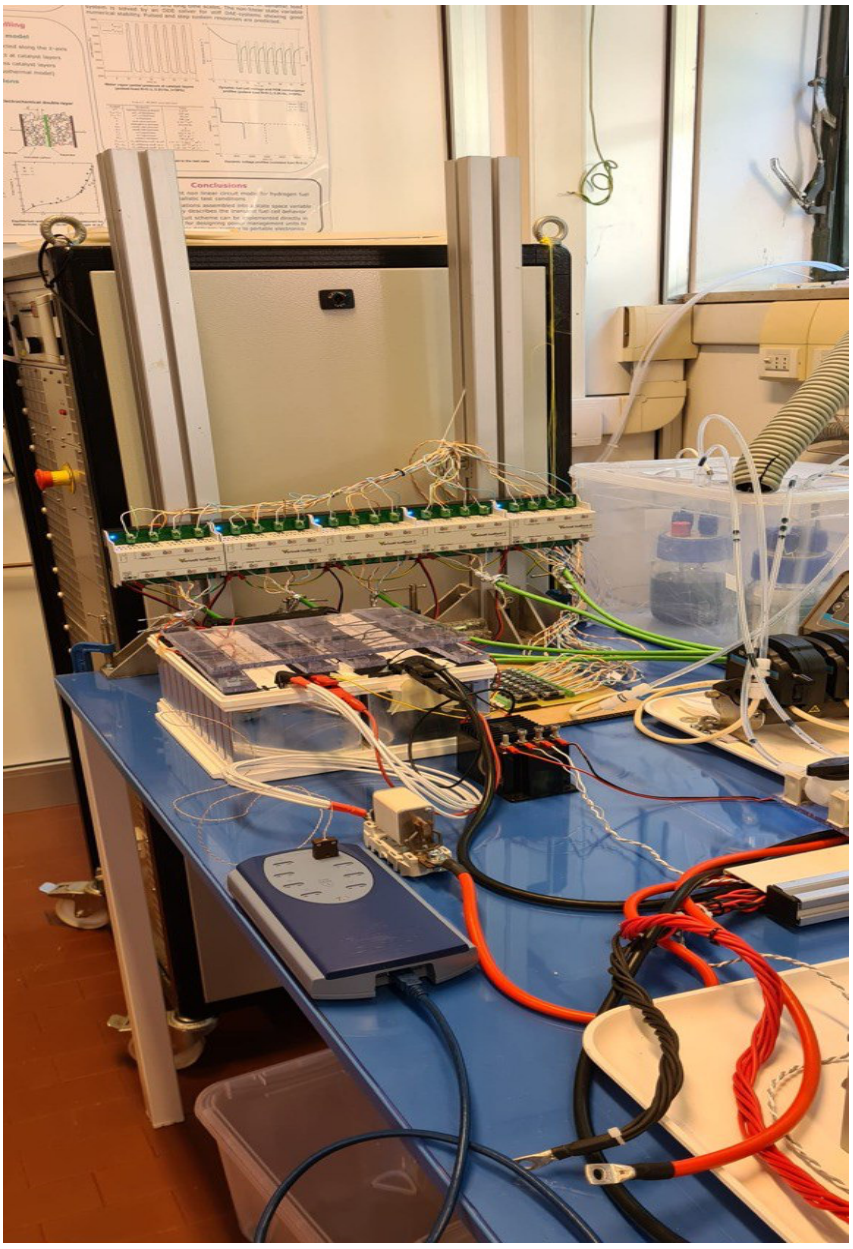

Fig 4_1

The currents and voltages measurements have been done with modules manufactured by National Instrument, the voltages of the module and of every individual cell have been measured. The temperature measurements have been done with eight type T thermocouples and with two thermo-resistors. The data were analyzed on the laboratory's pc which uses Labview.

The tests that have been executed are:

- Charge of the battery up to Vmax of the module of 54V, charge at constant current till V= Vmax and then constant voltage charge until the current decreased under 1A. With this test we wanted to confirm the correct behavior of the battery and of all the circuitry components. It has been found a remarkable difference between the cell voltages measured by the PC with the one measured with a multimeter, this problem is explained in the isoblock C-4c chapter.
- The battery has been charged and discharged to minimum 36V for two complete cycles. Between the charge and discharge, and vice-versa, it has been chosen a pause of exactly 1minute. With this test we analyzed the temperature's data measured through the resistance temperature detector and thermocouples.

The charge and discharge procedure were set by the PC, it has been chosen that when a single cell voltage exceed the maximum limit of 2.7V the whole charging procedure would stop and, vice versa, when the voltage fall below 1.5V during the discharge procedure. It has been arbitrary chosen that in those situations the battery would be considered fully charged or discharged respectively.

### *4.1 DSAC 85-75*

To charge and discharge the battery a linear power supplies manufactured by DANA has been used, it's made especially for testing uses and in particular for electrochemical devices to evaluate thermal behavior and to obtain charge and discharge waveforms of battery in cyclic way without disconnecting the battery from the power supply to connect it to a load [51]. The one used in laboratory can give a maximum Voltage of 85Vdc and current of 75A.

### *4.2 cDAQ ni9185*

The cDAQ-9185 is a compactDAQ Ethernet chassis for distributed sensor measurement system. The chassis controls: timing, synchronization and data transfer between C series modules and an external host. It's possible to combine C series modules to create a mix of analogue, digital and counter/timer measures. The cDAQ chassis is directly connected to the PC through Ethernet cable. C Series modules are automatically detected by the chassis and the I/O channels are accessible using the ni-DAQmx driver software. To perform analog input/output measurements it's needed a supported C Series Module into any slot of the cDAQ chassis, the number of channels, channel configuration, sample rate, gain, and others measurement specifications are determined by the type of C Series module used. The cDAQ chassis has three Analog Input timing engines, so three different analog input tasks can run at the same time, however channels from a single module cannot be used in multiple tasks. The sampling measure is done with a trigger signal, to start or stop the acquisition of data, and for this the cDAQ chassis supports internal software triggering, external

digital triggering, analog triggering and internal time triggering. To perform digital Input/Output (DIO) measurements a supported C Series module must be installed in any slot of the cDAQ chassis. The I/O specifications such as number of lines, logic levels, update rate, and line direction, are determined by the type of C Series module used. The triggering signals are the same for the Analog Input/output. Modules can be connected in serial or parallel. Serial module can perform software-timed and hardware-timed digital Input/Output tasks. Parallel digital modules can be used for software-timed and hardware-timed digital Input/Output tasks, counter/timer tasks, accessing PFI signal tasks and filter digital input signal. To choose which one of these two configuration is the better for the task it must be considered that software-timed and hardware-timed digital Input/Output tasks have the following restriction:

- You cannot use serial and parallel modules together on the same hardware-timed task
- You cannot use serial modules for triggering
- You cannot do both static and timed task at the same time on a single serial module
- You can only do hardware timing in one direction at a time on a serial bidirectional module

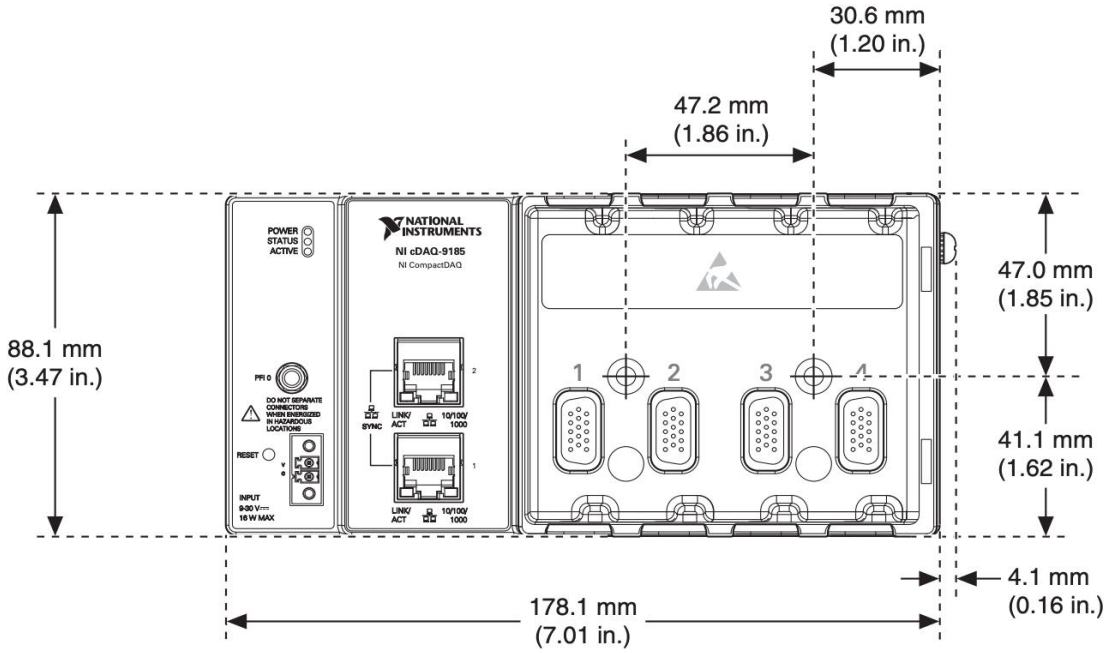


Fig 4_2

The Programmable Function Input (PFI) lines of the cDAQ-9185 chassis are designed for a cable length of 3 m indicating a cable impedance of 50 Ω and maximum input/output frequency of 1 MHz. In the reference [34] are specified the maximum operating conditions, if the cDAQ is stressed beyond these the chassis itself may be irreversibly damaged. The $I_{OL}$, the current flowing into the output at a specified low-level output voltage, maximum allowed is 8 mA, the $I_{OH}$, the current flowing into the output at a specified high-level output voltage [35], maximum allowed is -8 mA [34]. The Schmitt Trigger input characteristic are reported in the following table:

| Voltage | Minimum | Maximum |
|---|---|---|
| Positive-going threshold | 1.43 V | 2.28 V |
| Negative-going threshold | 0.86 V | 1.53 V |

| | | |
|---|---|---|
| Hysteresis | 0.48 V | 0.87 V |

Table 4_1

The source current is the ability of the digital output/input port to supply current, vice versa the sink current is the ability of the port to receive current. The characteristics are reported in the following table.

| Voltage | Conditions | Minimum | Maximum |
|---|---|---|---|
| High | - | - | 5.25 V |
| | Sourcing 100 $\mu$A | 4.65 V | - |
| | Sourcing 2 mA | 3.60 V | - |
| | Sourcing 3.5 mA | 3.44 V | - |
| Low | Sinking 100$\mu$A | - | 0.10 V |
| | Sinking 2mA | - | 0.64 V |
| | Sinking 3.5 mA | - | 0.80 V |

Table 4_2

The safety voltage is 30 V Maximum and the operating temperature T must be -40°C < T < 70°C. All the previous value are determined at a room temperature of 25°C. The voltage input range, measured at the chassis power connector, is from 9 V to 30 V, while the maximum power consumption is 16 W [34].

### *4.3 ni-9217*

The ni-9217 is C series module compatible with the cDAQ-9185 chassis, it's a resistance temperature detector (RTD) input module with a resolution of

24 bit and has four analog input channels in total. The ni-9217 is compatible with 3 and 4-wire RTD sensors, it automatically recognizes the type RTD type and adjust accordingly to the appropriate mode. The thermo-resistor used are PT100 and means that it's made in platinum and has a resistance of 100 Ω at 0°C with a sensibility of ± 0.1 °C. The thermo-resistance were placed in the inner cells of the battery as shown in Fig 4_3.

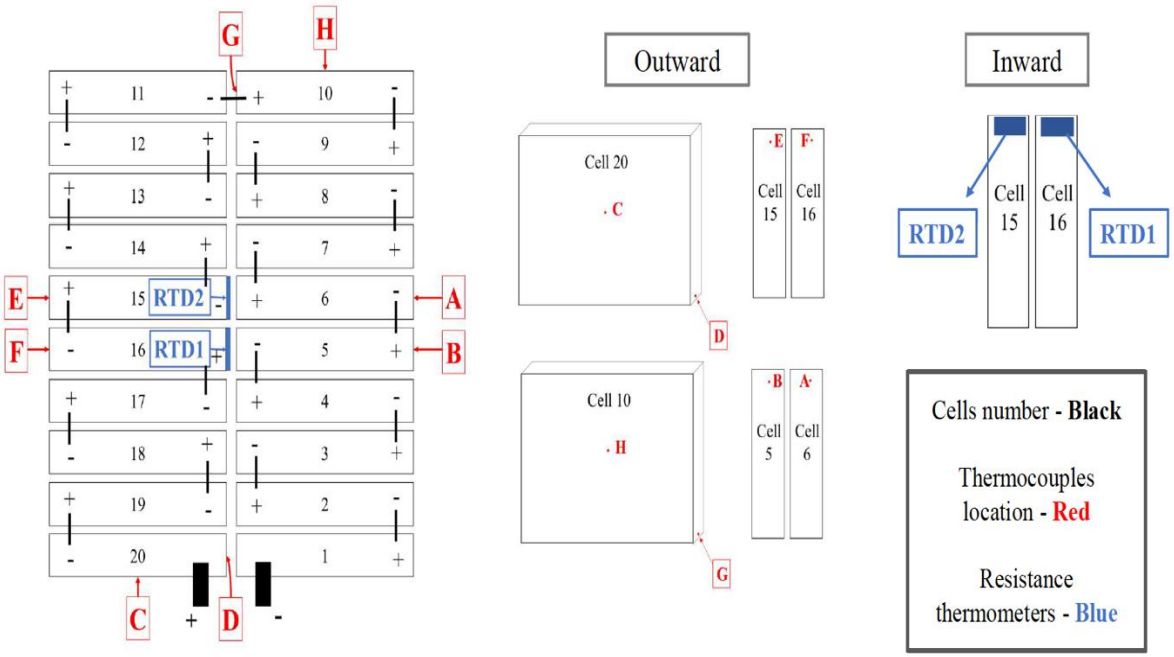


Fig 4_3

The measurement range is:

- For Temperature from -200 °C to 850 °C
- For Resistance from 0 Ω to 400 Ω

During operation the voltage must remain limited under ± 30 V.

Fig4_4 shows the input circuitry of the module.

As can be seen from the figure RTD channels of the module share a common ground that is isolated from other modules of the system.

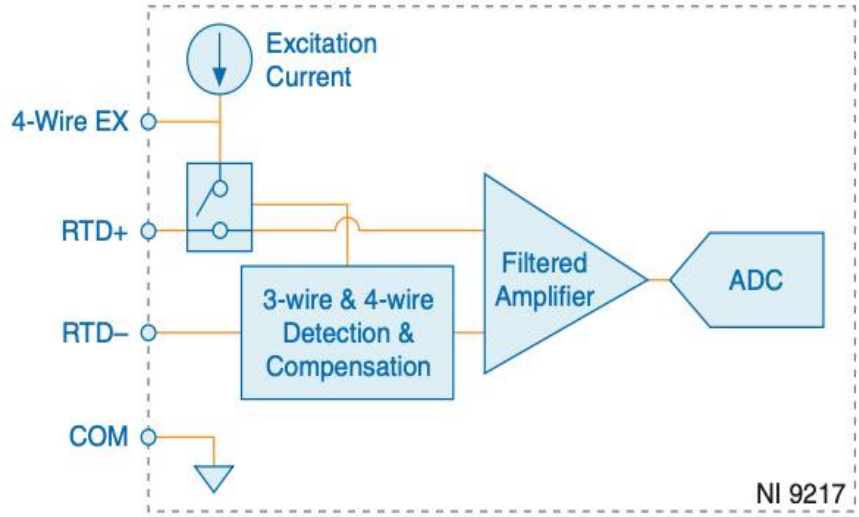

Fig 4_4

### *4.9 TC-08*

The temperature analysis and data measurement have been done with TC-08 manufactured by PICO [50]. Each unit has a total of eight channel for different thermocouples and each measure has an accuracy equal to the sum of ±0.2% of the measure plus ±0.5°C. The thermocouples compatible are: B, E, J, K, R, S, and the one used the T type which are in costantan, a copper-nickel alloy, and are able to operate in a range of temperature form -200°C to +400°C.

### *4.4 ni-9207*

The ni-9207 is a C series module with a total of sixteen analog input channels, eight for currents and 8 for voltages, with a resolution of 24 bits. The module maximum limits are:

- 10.4 V for each voltage channel
- 21.5 mA for each current channel

And every channel has a voltage and current input impedance, respectively of 1 GΩ and 85 Ω. Every voltage channel must remain within ±10.2 V channel-to-COM, this identifies the maximum working voltage for analog input. The current channels can withstand a maximum current of 2 A and voltage up to 30 V while the entire module has an overvoltage protection, measured channel-to-COM and for each Individual channel, of ±30 V maximum on one channel at a time. The module has been used for the measures of currents and for the measurement of the voltage of four cells and of the entire module. Since the module can directly only do voltage measurements a current transducer is needed, the one used is the DS50ub-10V. The entire module has a total voltage 54 V far much greater than the 10.2 V allowed for channel; to proceed with the measure a Lem cv3-100/sp voltage transducer has been inserted in series, which after measuring, sends a proportional value to the ni-9207.

Fig 4_5 shows the input circuitry of the module.

The input signals are scanned, amplified, conditioned, and then sampled by a single 24-bit ADC.

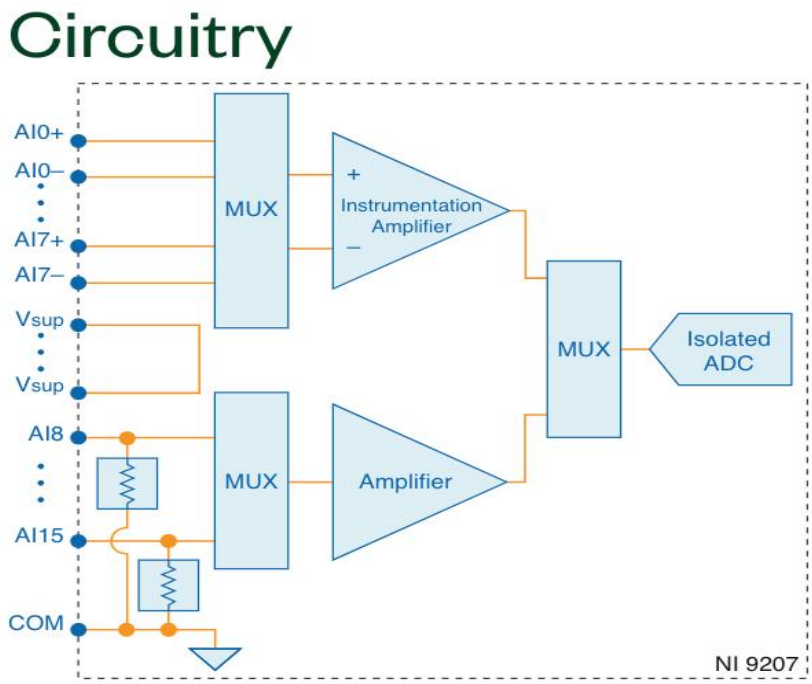

Fig 4_5

### *4.5 DS50ub-10V*

It's an ultra-stable, high precision current transducer for non-intrusive, isolated DC and AC current measurement. It's able to measure currents up to nominal value of 50 A in DC, which is the case that has been used for, giving a nominal output voltage of 10 V at nominal current, the ratio is 5A: 1V. When operating with AC values the amplitude error increases with the increasing of the frequency with a max error of 3% for frequency in between 10kHz and 100kHz [32].

### *4.6 CV3-100/SP3*

This component is a Voltage Transducer made by LEM, for DC and AC voltages. It has measurement range of 0…±130V in input and has a conversion ratio of 20, 100V: 5V and it's used to measure the voltage of the total module, it sends the output signals to the 9207 module. The following figure shows the connection scheme.

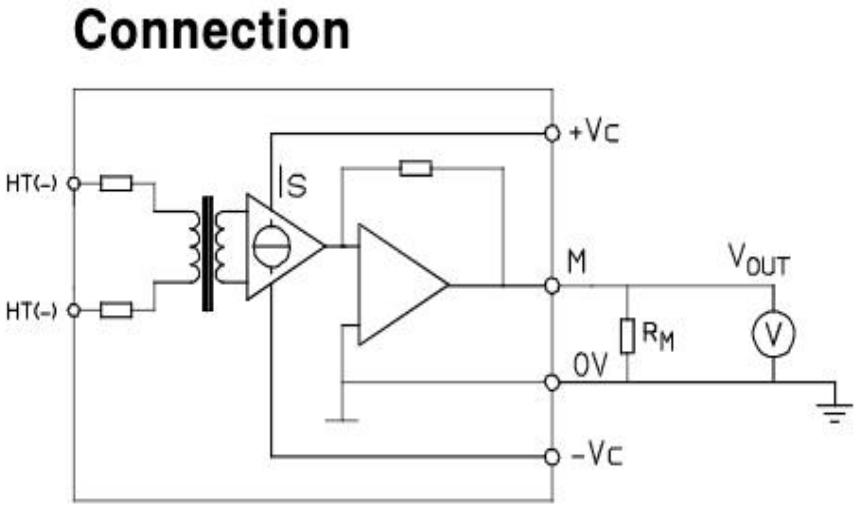


Fig 4_6

### *4.7 ni-9209*

The ni-9209 is voltage input a C series module is used to take data about the voltage of the remaining sixteen cells of the stack. The module has a total of differential channels and each channel must remain within ±10.4V. The voltages are measured as signal voltage + common mode voltage and thus the voltage is not floating, the first channel measures the 2.4V of the first cell while the last one measures the voltage o the sum of the previous sixteen cells, value that far exceed the maximum limit of 10.4V. fig. shows the input circuitry of the module [48].

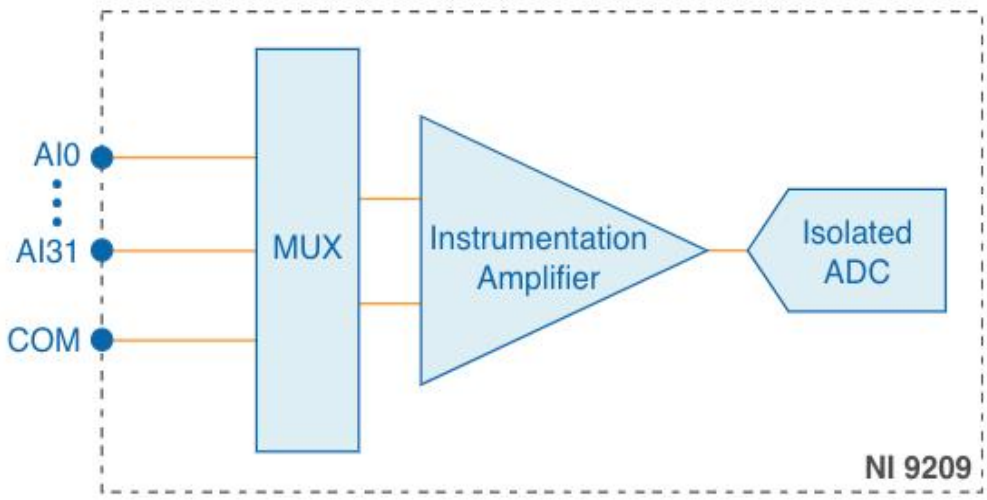

Fig 4_7

To solve this problem, it's used the isoblock C-4c galvanic insulator manufactured by Verivolt.

### *4.8 Isoblock C-4c*

This module, manufactured by Verivolt, has been designed to provide high quality and low-cost differential voltage measurements along a chain of batteries. Each module has four separated isolated channels for four different measurement sources with a maximum input voltage limit of $\pm$ 30V. The module measure for each channel the voltage in respect to earth and to lower the input voltage value a voltage divider has been inserted, unluckily the used resistances were of too high value, of the order of 100kΩ, and thus the parallel of the resistances measured by the PC gave a lower value than the one obtained with a multimeter. For the future works it should be tried substituting these resistances with others of the others of kΩ.

# 6 Conclusion

Considering the role that energy storage will have in the coming years in helping the spread of renewable energies, interest in the different types of energy storage technologies is growing. Redox Flow Batteries RFB are gaining more and more popularity due to their advantages in being used as batteries for stationary applications, especially in sizes of several kW or even MW and with long discharge times (>4 hours). The first part of the work done in this thesis focuses on the safety aspects of the operation of a VRFB. Firstly, an industrial size VRFB "IS-VRFB" with a 9 kW / 27 kWh that is in operation at the Electrochemical Energy Storage and Conversion Laboratory (EESCoLab) has been analyzed regarding safety issues. It is shown that with an appropriate design, in the presence of a dangerous event, all the static protective measures are in place to contain the risks, while the necessary active measures are only the isolation and / or shutdown of the battery system in the presence of failure or malfunction of a sensor. Regarding lithium-ion batteries it has been shown that when a thermal runaway occurs there is a high risk of propagation, the phenomenon can only be contained and not stopped once it occurs. Current studies try to propose security control systems or models to identify in advance the onset of this disruptive phenomenon, there are promising studies but at the moment none have shown definitive results. For this reason, this study focused mainly on the test procedures required by the standards and on the tests that the battery manufacturer must carry out to ensure at least a certain level of stability intrinsic to abuse and safety of thermal behavior. Both for flow batteries and for lithium batteries it has been shown the fundamental importance of the battery housing both to contain any leaks, gas production and contain the initial

spread of a fire. Since, fire risk and personnel safety are paramount considerations when designing, permitting and operating large energy storage systems, it can be concluded that VFBs are among the safest storage technologies on the grid today, in comparison with Li-ion batteries. In the second part of this thesis an experimental analysis of an in-house designed “Li-ion battery test facility” has been carried out. It is capable of testing a 48 V Li-ion battery pack composed by 20 cells electrically connected in series with a nominal capacity of 20 Ah. A preliminary experimental campaign has been performed at the aim to demonstrate the feasibility of this system. This experimental work has been done within a technology transfer contract between FIAMM Energy Technology and EESColab.

# TABLE INDEX

# FIGURES INDEX

# BIBLIOGRAPHY


[1] 2005, IEC 60364-4-41, “protection against electro-shock”

[2] 2011, CEI 99-3, “grounding system for electrical system with nominal voltage higher than 1 kV”

[3] 2020, IEC 62932-2-2, “Flow battery system for stationary application part 2-2: safety requirements”

[4] Angorro B., Yatadhia R.E., “The grounding Impedance Characteristics of Grid Configuration”, Elsevier, 2013

[5] Mirsajed Pourmirasghariyan, Seyed Fariborz Zarei, Mohsen Hamzeh, “DC-system grounding: Existing strategies, performance analysis, functional characteristics, technical challenges, and selection criteria - a review”, Electric Power Systems Research (206), 2022

[6] Haize Hu[a] Richeng Luo, Mengge Fang, Shuiling Zeng, Feiyu Hu, “A new optimization for grounding grid”, Electrical power and Energy systems (108), 2019

[7] 2015, IEC 62485-1, “Safety requirements for secondary battery and battery installations part 1: general safety information”

[8] 2018, IEC 62485-2, “Safety requirements for secondary battery and battery installations part 2: stationary batteries”

[9] 2019, IEC 60364-5-53, “electrical installation of buildings- part 5-53: selection and election of electrical equipment- isolation, switching and control”

[10] 2020, IEC 62932-2-1, “Flow battery system for stationary application part 2-1: general requirements and testing methods”

[11] A.H. Whitehead, T.J. Rabbow, M. Trampert, P. Pokorny, “critical safety features of the vanadium redox flow battery”, journal of Power Sources, 2017

[12] 2019, CEI 0-16, “regola tecnica di riferimento per la connessione di Utenti attivi e passivi alle reti AT e MT delle imprese distributrici di energia elettrica”

[13] 2019, CEI 0-21, “regola tecnica di riferimento per la connessione di Utenti attivi e passivi alle reti BT delle impese distributrici dell’energia elettrica

[14] 2007, CEI 64-8, “Impianti elettrici utilizzatori a tensione nominale non superiore a 1000V in a.c. e 1500V in d.c.”

[15] 2012, ISO 7010, “segnaletica di sicurezza”

[16] 2007, Voltimum, “sistemi a bassissima tensione”, available: https://www.voltimum.it/sites/www.voltimum.it/files/fields/attachment_file/it/attachments/gii/r/scheda_selv_felv_pelv_05_07_07.pdf

[17] 2004, Voltimum, “impianto di terra”, available:
Part1:
https://www.voltimum.it/sites/www.voltimum.it/files/it/attachments/pdi/f/pdf/040311_impianto-terra1.pdf
Part2:
https://www.voltimum.it/sites/www.voltimum.it/files/it/attachments/pdi/f/pdf/040312_impianto-terra2.pdf

[18] UNAE, “impianti di terra”, available:
https://veneto.unae.it/wp-content/uploads/sites/6/2020/09/N.13-Gli-Impianti-di-terra-18-9-2020.pdf
(consulted in data 3/02/2022)

[19] Amelio Faccini, “Atmosfere potenzialmente esplosive”, available:
https://it.scribd.com/document/385328906/Classificazioni-Atex
(consulted in data 20/03/2022)

[20] 2013, “Rischio di esplosione, misure di protezione e implementazione delle Direttive ATEX 94/9/CE e 99/92/CE”, INAIL

[21] 2011, CEI 31-35, “Atmosfere esplosive per la presenza di gas-classificazione dei luoghi, Guida all’applicazione della norma CEI EN 60079_10-1 (CEI 31-87):2010-1”

[22] 2018, “Scheda di sicurezza-acido solforico”, FIAMM

[23] Qingsong Zhang, Jianghao Niu, Ziheng Zhao, Qiong Wang, “Research on the effect of thermal runaway gas components and explosion limits of lithium-ion batteries under different charge states”, Journal of Energy Storage, 2022

[24] Yuqing Chen, Yuqiong Kang, Yun Zhao, Li Wang, Jilei Liu, Yanxi Li, Zheng Liang, Xiangming He, Xing Li, Naser Tavajohi, Baohua Li, “A review of lithium-ion battery safety concerns: The issues, strategies, and testing standards”, Journal of Energy Chemistry, 2021

[25] Pengjie Liua, Chaoqun Liub, Kai Yangb, Mingjie Zhangb, Fei Gaob, Binbin Maoa, Huang Lia, Qiangling Duana, Qingsong Wanga, “Thermal runaway and fire behaviors of lithium iron phosphate battery T induced by over-heating”, Journal of Energy Storage, 2020

[26] Dongsheng Ren, Xuning Feng, Languang Lu, Minggao Ouyang, Siqi Zheng, Jianqiu Li, Xiangming He, “An electrochemical-thermal coupled overcharge-to-thermal-runaway model for lithium ion battery” Journal of Power Sources, 2017

[27] Fei Gao et al., “Study on Temperature Change of LiFePO /C Battery Thermal Runaway under Overcharge Condition”, 3rd International Conference on Air pollution and Environmental

Engineering, 2021

[28] Hao Ji, Yi-Hong Chung, Xu-Hai Pan, Min Hua, Chi-Min Shu, Li-Jing Zhang, “Study of lithium-ion battery module’s external short circuit under different temperatures”, Journal of Thermal Analysis and Calorimetry, 2021

[29] Shan Huang, Xiaoniu Du, Mark Richter, Jared Ford,1Gabriel M. Cavalheiro, Zhijia Du, Robin T. White, and Guangsheng Zhang, “Understanding Li-Ion Cell Internal Short Circuit and Thermal Runaway through Small, Slow and In Situ Sensing Nail Penetration”, Journal of The Electrochemical Society, 2020

[30] Shan Huang and Guangsheng Zhang, “Understanding Li-Ion Battery Thermal Runaway through Small, Slow and in Situ Sensing Nail Penetration”, The Electrochemical Society, 2020

[31] Zonghou Huang, Huang Li, Wenxin Mei, Chunpeng Zhao, Jinhua Sun and Qingsong Wang, “Thermal Runaway Behavior of Lithium Iron Phosphate Battery During Penetration”, Fire Technology, 2020

[32] Life Energy motion LEM, “CV3-100/SP3 datasheet”, available at: https://www.lem.com/sites/default/files/products_datasheets/cv_3-100_sp3.pdf

[33] National Instruments, “cDAQ-9185-9189 user manual”, available at:
https://www.ni.com/docs/en-US/bundle/cdaq-9185-9189-features/resource/376610b.pdf

[34] National Instruments, “cDAQ-9185 specifications”, available at:
https://www.ni.com/docs/en-US/bundle/cdaq-9185-specs/page/specs.html

[35] 2014, “TERMS, DEFINITIONS, ABBREVIATIONS, SYMBOLS AND UNITS FOR INTEGRATED CIRCUITS”, available at:
http://escies.org/escc-specs/published/2139000.pdf

[36] National Instruments, “ni-9217 datasheet”, available at:
https://www.ni.com/docs/en-US/bundle/ni-9217-specs/resource/374187a_02.pdf

[37] National Instruments, “ni-9207 datasheet”, available at:
https://www.ni.com/docs/en-US/bundle/ni-9207-specs/page/overview.html

[38] National Instruments, “ni-9207 specifications”, available at:
https://www.ni.com/docs/en-US/bundle/ni-9207-specs/page/specifications.html

[39] Eduardo Sa´nchez-Díeza, Edgar Ventosab, Massimo Guarnieri, Andrea Trovò, Cristina Flox, Rebeca Marcilla, Francesca Soavi, Petr Mazur, Estibaliz Aranzabe, Raquel Ferreta, “Redox flow

batteries: Status and perspective towards sustainable stationary energy storage", Journal of Power Sources, 2021

[40] Álvaro Cunha, Jorge Martins, Nuno Rodrigues and F. P. Brito, "Vanadium redox flow batteries: a technology review", International Journal of Energy Research",2014

[41] Puiki Leung,a Xiaohong Li, Carlos Ponce de Leo, Leonard Berlouis, C. T. John Lowa and Frank C. Walshab, "Progress in redox flow batteries, remaining challenges and their applications in energy storage", RSC advances, 2012

[42] Aishwarya Parasuramana, Tuti Mariana Lima, Chris Menictasc, Maria Skyllas-Kazacosc "Review of material research and development for vanadium redox flow battery applications", Electrochimica Acta, 2013

[43] Adam Z. Weber, Matthew M. Mench, Jeremy P. Meyers, Philip N. Ross,Jeffrey T. Gostick, Qinghua Liu, "Redox flow batteries: a review", Journal of Applied Electrochemistry, 2011

[44] Cong Ding, Huamin Zhang, Xianfeng Li, Tao Liu, and Feng Xing, "Vanadium Flow Battery for Energy Storage: Prospects and Challenges", American Chemical Society, 2013

[45] Danisense, “DS50ub-10V datasheet”, https://danisense.com/wp-content/uploads/DS50UB-10V.pdf

[46] National Instruments, “ni-9209 datasheet”, available at: https://www.ni.com/docs/en-US/bundle/ni-9209-specs/page/overview.html

[47] National Instruments, “ni-9209 specifications”, available at: https://www.ni.com/docs/en-US/bundle/ni-9209-specs/page/specifications.html

[48] Verivolt, “isoblock C-4c datasheet and specs”, available at: https://www.verivolt.com/web/content/15005/IsoBlock%20C%20specsheet.pdf

[49] PICO, “TC-08 datasheet”, available at: https://www.farnell.com/datasheets/2630545.pdf?_ga=2.143841653.1797568111.1580333416-1061579168.1558457094

[50] Danasrl, “DSAC linear power supplies specs”, available at: http://www.danasrl.it/images/prodotti/SERIE%20-%20D2AC.pdf